Diagnostic quality in computed tomography angiography after EVAR

Lehti, Leena

2019

Document Version:
Publisher's PDF, also known as Version of record

Diagnostic quality in computed tomography angiography after EVAR

LEENA LEHTI
DEPARTMENT OF DIAGNOSTIC RADIOLOGY | LUND UNIVERSITY

Diagnostic quality in computed tomography angiography after EVAR

Leena Lehti

LUND UNIVERSITY

DOCTORAL DISSERTATION

by due permission of the Faculty Medicine, Lund University, Sweden.
To be defended at Lilla Aulan, SUS Malmö, June 13th 2019 at 9 am.

Faculty opponent
Professor Lars Lönn, MD PhD, University of Copenhagen

Organization	Document name
LUND UNIVERSITY Department of Diagnostic Radiology, Clinical Sciences Lund, Faculty of Medicine	DOCTORAL DISSERTATION
	Date of issue 13th June 2019
Author(s) Leena Lehti	Sponsoring organization

Diagnostic quality in computed tomography angiography after EVAR

Abstract

Background: Follow-up of endovascular aortic aneurysm repair (EVAR) with life-long computed tomography angiography (CTA) surveillance exposes patients with impaired renal function to repeated high doses of iodine contrast medium and significant levels of radiation. Endoleaks are complications after EVAR that can be treated with Onyx® causing severe artefacts in CTA follow-up impairing diagnostic reliability.

Aims: The specific aims of this thesis were to:

- Assess image quality in CTA after EVAR with halved contrast medium dose in azotemic patients using 80-kVp CT technique (paper I).
- Compare image quality of virtual non-contrast (VNC) images reconstructed from arterial (paper II) or both arterial and venous phase (paper III) dual-energy CTA to true non-contrast (TNC) images, and assess whether they can replace TNC images.
- Assess whether post-processing of CTA images using iterative metal artefact reduction can reduce severe artefacts caused by Onyx®, and improve diagnostic quality compared to standard image reconstructions (paper IV).

Material and methods: A total of 80 patients (40 with 80-kVp technique and 40 with 120-kVp technique) were studied after EVAR, and CT image quality was assessed (paper I). Thirty patients with suspected aortic aneurysm, aortic dissection, or undergoing subacute control after EVAR were examined with dual-energy CT. VNC images were reconstructed from the arterial phase scan. Attenuation values, image noise, and subjective image quality were assessed (paper II). Sixty-three patients were examined with dual-energy CTA at EVAR follow-up. Attenuation values and images noise were assessed in VNC images reconstructed both from arterial and venous phase scans, and compared to those in TNC images (paper III). Twelve patients were examined with dual-energy CTA after Onyx® embolization of type 2 endoleaks following EVAR. A standard image dataset without iMAR and eight image datasets with different iMAR algorithms were reconstructed per patient. Attenuation values and image noise were measured in aorta or iliac arteries and muscle tissue close to Onyx®, and compared to a reference level at the diaphragm. Subjective image quality and severity of artefacts were assessed (paper IV).

Results:

- 80-kVp technique with halved contrast media dose may provide satisfactory diagnostic results for CTA follow-up of EVAR compared to common standards, and lower the risk of contrast medium induced nephropathy (CIN) in patients with BMI below 35 kg/m^2 (paper I).
- VNC images reconstructed from arterial phase CTA scans are not suitable replacements for TNC images (paper II). VNC images reconstructed from venous phase CTA scans, on the other hand, can more accurately replace TNC images (paper III).
- iMAR algorithms can significantly reduce metal artefacts and improve diagnostic quality in CTA in patients treated with Onyx® for endoleaks following EVAR (paper IV).

Conclusion: New CT techniques and image reconstruction methods can improve patient safety and reduce radiation doses with maintained or even improved image quality.

Keywords

Abdominal aortic aneurysm, EVAR, computed tomography angiography, contrast medium induced nephropathy, dual-energy computed tomography, image reconstruction, attenaution values, metal artefact reduction.

Classification system and/or index terms (if any)

Supplementary bibliographical information		**Language** Enlish
ISSN and key title 1652-8220		**ISBN 978-91-7619-2**
Recipient's notes	**Number of pages 65**	Price
	Security classification	

Signature  Date 2019-04-24

Diagnostic quality in computed tomography angiography after EVAR

Leena Lehti

LUND
UNIVERSITY

Cover image by Laura Kalbag, Ind.ie

Faculty of Medicine
Institution of Clinical Sciences, Lund
Department of Diagnostic Radiology

ISBN 978-91-7619-791-2
ISSN 1652-8220

Printed in Sweden by Media-Tryck, Lund University
Lund 2019

Media-Tryck is an environmentally certified and ISO 14001:2015 certified provider of printed material. Read more about our environmental work at www.mediatryck.lu.se

MADE IN SWEDEN

To Olivia and Max

Table of contents

Abbreviations

ALARA	as low as reasonably achievable
CIN	contrast medium induced nephropathy
CNR	contrast to noise ratio
CTA	computed tomography angiography
CTDI	computed tomography dose index
DECT	dual-energy computed tomography
DLP	dose length product
EVAR	endovascular aortic aneurysm repair
GFR	glomerular filtration rate
HU	Hounsfield units (attenuation)
iMAR	iterative metal artefact reduction algorithm
kVp	peak kilovoltage (tube voltage)
mA	milliampere (tube current)
mAs	milliampere seconds (tube load)
mGy	milligray (radiation absorbed dose)
mSv	millisievert (radiation effective dose)
ROI	region of interest
SD	standard deviation
TNC	true non-contrast
VNC	virtual non-contrast

Original papers

I. 80-kVp CT angiography for endovascular repair follow-up with halved contrast medium dose and preserved diagnostic quality.

Leena Lehti, Ulf Nyman, Marcus Söderberg, Katarina Björses, Anders Gottsäter, Johan Wasselius. Acta Radiologica, 2016 March 57(3):279-86.

II. Reliability of virtual non-contrast computed tomography angiography: comparing it with the real deal.

Leena Lehti, Marcus Söderberg, Peter Höglund, Ulf Nyman, Anders Gottsäter, Johan Wasselius. Acta Radiologica Open, 2018 August 7(7-8) 2058460118790115.

III. Comparing arterial- and venous-phase acquisition for optimization of virtual non-contrast images from dual energy computed tomography angiography.

Leena Lehti, Marcus Söderberg, Peter Höglund, Johan Wasselius. In manuscript.

IV. Metal artefact reduction in aortic computed tomography after EVAR and Onyx®-embolization.

Leena Lehti, Marcus Söderberg, Peter Höglund, Johan Wasselius. In manuscript.

Summary

Follow-up of endovascular aortic aneurysm repair (EVAR) with life-long computed tomography angiography (CTA) surveillance exposes patients with impaired renal function to repeated high doses of iodine contrast medium and significant levels of radiation. Endoleaks are complications after EVAR that can be treated with Onyx® causing severe artefacts in CTA follow-up impairing diagnostic reliability.

The specific aims of this thesis were to:

- Assess image quality in CTA after EVAR with halved contrast medium dose in azotemic patients using 80 kVp CT technique (paper I).
- Compare image quality of virtual non-contrast images reconstructed (VNC) from arterial (paper II) or both arterial and venous phase (paper III) dual-energy CTA to true non-contrast images (TNC), and assess if they are suitable to replace TNC images.
- Assess whether post-processing of CTA images using iMAR algorithms can reduce severe artefacts caused by Onyx®, and improve diagnostic quality compared to standard image reconstructions (paper IV).

A total of 80 patients (40 with 80 kVp technique, 40 with 120 kVp technique) were studied after EVAR, and CT image quality was assessed (paper I). Thirty patients with suspected aortic aneurysm, aortic dissection, or undergoing subacute control after EVAR were examined with dual-energy CT. VNC images were reconstructed from the arterial phase scan. Attenuation values, image noise, and subjective image quality were assessed (paper II). Sixty-three patients were examined with dual-energy CTA at EVAR follow-up. Attenuation values and images noise were assessed in VNC images reconstructed both from arterial and venous phase scans, and compared to those in TNC images (paper III). Twelve patients were examined with dual-energy CTA after Onyx® embolization of type 2 endoleaks following EVAR. One standard image dataset without iMAR and eight image datasets with different iMAR algorithms were reconstructed per patient. Attenuation values and image noise were measured in the aorta or iliac arteries and muscle tissue close to the Onyx®, and were compared to a reference level at the diaphragm. Subjective image quality and severity of s were assessed (paper IV).

Results:

- 80 kVp technique with halved contrast media dose for CTA follow-up of EVAR may provide satisfactory diagnostic results compared to common standards, and lower the risk of contrast induced nephropathy (CIN) in patients with BMI below 35 kg/m2 (paper I).
- VNC images reconstructed from arterial phase CTA scan are not suitable replacements for TNC images (paper II). VNC images reconstructed from venous phase CTA scan, on the other hand, can more accurately replace TNC images (paper III).
- The iMAR algorithms can significantly reduce metal artefacts and improve diagnostic quality in CTA in patients treated with Onyx® for endoleaks following EVAR (paper IV).

In conclusion, new CT techniques and image reconstruction methods can improve patient safety and reduce radiation dose with maintained or even improved image quality.

Introduction

The aorta is the main artery of the body, ascending from the heart and supplying oxygenated blood to all body organs via its branches. An abdominal aortic aneurysm (AAA), a dilatation of the abdominal aorta, is defined as a maximal infrarenal aortic diameter of 30 mm or more, representing a 50% increase of the normal (20 mm) maximal abdominal aortic diameter (1, 2). Dilatation of the aorta gradually leads to weakening of the aortic wall, a process which might lead to rupture if left untreated. This dilatation process is usually asymptomatic.

Endovascular aortic aneurysm repair (EVAR) is a minimally invasive surgical method for treatment of abdominal aortic aneurysms. A stent graft is deployed through femoral access inside the aneurysm, excluding the aneurysm sac from the blood circulation. Rapid development of endovascular techniques and materials during the last two decades have enabled this treatment for larger numbers of patients. Potential advantages of EVAR compared to open aneurysm repair include reduced operative time, less surgical trauma and post-operative pain, and reduced length of stay in both hospital wards and intensive care units (3-6). The method also has disadvantages, however, including immediate and late complications such as incomplete aneurysm sac sealing, with continuous refilling of the aneurysm sac or backfilling of the aneurysm from small vessels in the aneurysm wall (7). To monitor such potential complications after EVAR, patients usually need to undergo repetitive evaluations with contrast computed tomography angiography (CTA), the most reliable imaging technique (8).

A major drawback of serial CTA, however, is the risk of contrast medium induced nephropathy (CIN) (9, 10). Patients undergoing EVAR quite commonly have several different risk factors for CIN; impaired renal function, diabetes mellitus, and congestive heart failure. Furthermore, repetitive imaging with CTA in EVAR patients exposes them to cumulative doses of radiation.

Abdominal aortic aneurysm

Definition, diagnosis, epidemiology and screening

An abdominal aortic aneurysm (AAA) is a dilatation of the infrarenal aorta, which has a multifactorial etiology featuring proteolytic enzymes causing chronic weakening of the arterial wall, inflammatory processes, and many of the classical risk factors for atherosclerosis. It is defined as a dilatation of the aorta 1.5 times the normal size or more, or as an aortic diameter of ≥ 30 mm in anterior-posterior measurement. The diameter of the aneurysm is a significant and independent risk factor for AAA rupture (11).

Table 1.
12- month AAA rupture risk by aortic diameter.

AAA diameter (mm)	Annual rupture risk (%)
30-39	0
40-49	1
50-59	1-11
60-69	10-22
>70	30-33

In most cases, an AAA is asymptomatic and the disease might therefore progress over many years before it is diagnosed. The aneurysm is often found *en passant* at an unrelated radiological examination, or by detecting a pulsatile mass in the abdomen at physical examination of the patient.

Abdominal ultrasound has both high sensitivity and specificity for detection of AAA, and is therefore used as a screening method in both several European countries and the United States (12-14). This study method provides an accurate measurement of the infrarenal aortic diameter, and allow detection of aortic wall lesions and mural thrombus. Furthermore it is painless, not dependent on ionizing radiation, and carries low costs. An AAA diagnosis with ultrasound is performer-dependent, however, and does not provide the detailed anatomical information needed to establish the optimal treatment of the aneurysm.

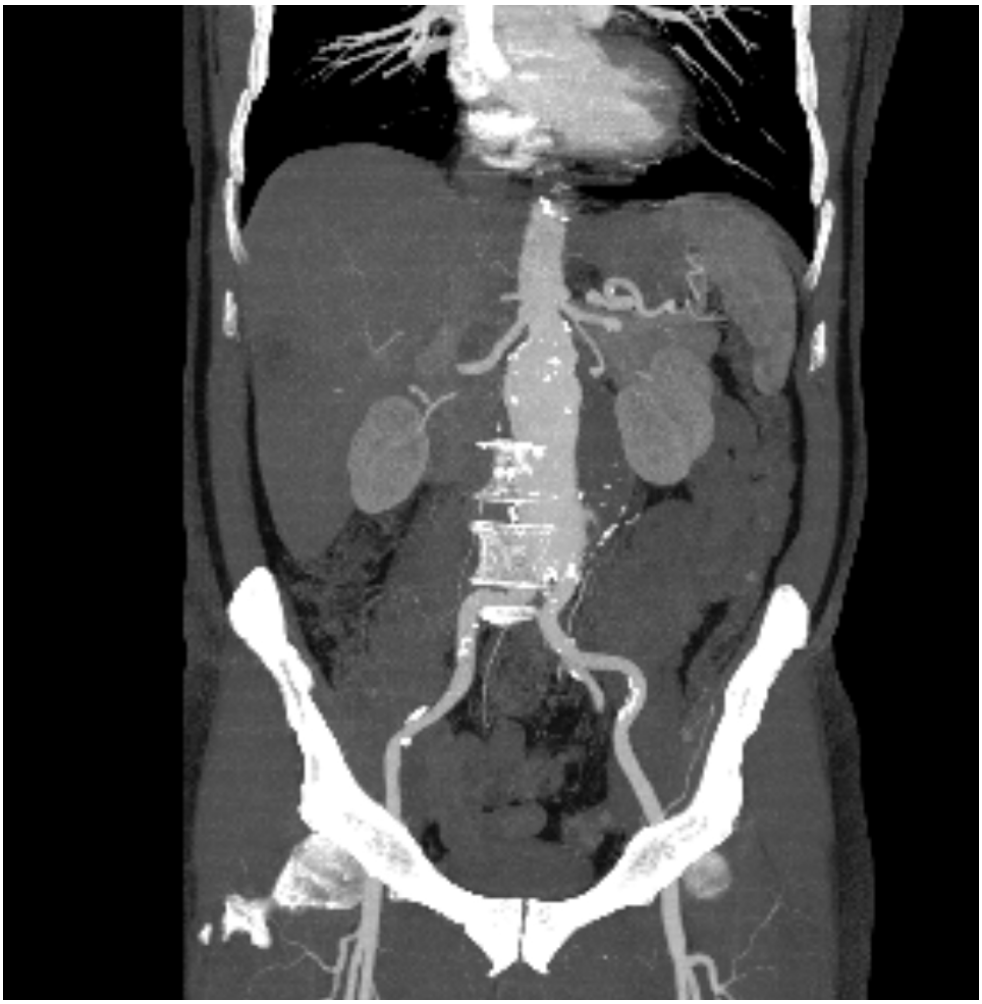

Figure 1.
CT angiography reveals the aortic anatomy in details.

Contrast enhanced CTA is the most common imaging method for thorough evaluation of aortic anatomy and morphology, and provides the detailed information needed to plan operative aortic repair (11, 15-22). One of the major drawbacks of CTA is the need for administration of iodinated contrast agent, which can cause both CIN and allergic reactions (9, 23). The use of ionizing radiation may also limit the use of the method, especially in younger patients needing serial radiological follow-up.

Magnetic resonance angiography (MRA) of the aorta provides highly detailed information on anatomical features and blood flow properties, but the use of the

method is limited by its high costs and lower availability compared to CTA (24). The drawbacks of MRA are difficulties to use the method in unstable or restless patients, and the contraindication for use in patients with pacemakers or ferromagnetic metal implants. On the other hand, MRA does not require ionizing radiation and is therefore suitable for serial follow-up studies in younger patients with known aortic disease.

Risk markers for development of AAA are advanced age, male gender, cigarette smoking, family history, arterial hypertension, hypercholesterolemia, and other cardiovascular diseases such as coronary artery disease or cerebrovascular disease (25).

With declining autopsy rates, population-based screening programs for AAA are now the most reliable way to estimate AAA prevalence. In the four randomized trials of AAA screening, aneurysm prevalence varied between 4.0% and 7.6% in men, and was estimated to 1.3% in women (12-14, 26). As 400 to 500 deaths in men $\geq$ 65 years of age were annually attributed to ruptured AAA in Sweden, a nationwide AAA screening program was started in 2006. The Swedish Aneurysm Screening Study group has integrated the screening system into the existing public healthcare system, and coordinates scientific projects related to the program. Today all Swedish men aged 65 years are consecutively identified through the national population registry, and invited to ultrasound examination of the abdominal aorta (27), regardless of whether they have any previously known AAA or not.

Indications for treatment

According to recommendations from the European Society of Cardiology, men with an AAA size of 5.5 cm and women with an AAA size of 5.0 cm should be referred to a vascular surgeon for evaluation concerning operative treatment (8).

Endovascular treatment

The first successful EVAR was completed by Nicholas Volodos in 1987, and thereafter Parodi and Palmaz published their first experiences in Argentina in 1991 attracting more attention to this less invasive treatment method (28, 29). In the standard EVAR technique, the main stentgraft part is introduced from one femoral artery using Seldinger (30) technique and stiff guidewires with positioning of the fabric-covered part of the stentgraft just below the renal arteries under fluoroscopy. The main stentgraft has one leg extending to the common hypogastric artery, which usually must be combined with another leg introduced from the contralateral femoral artery.

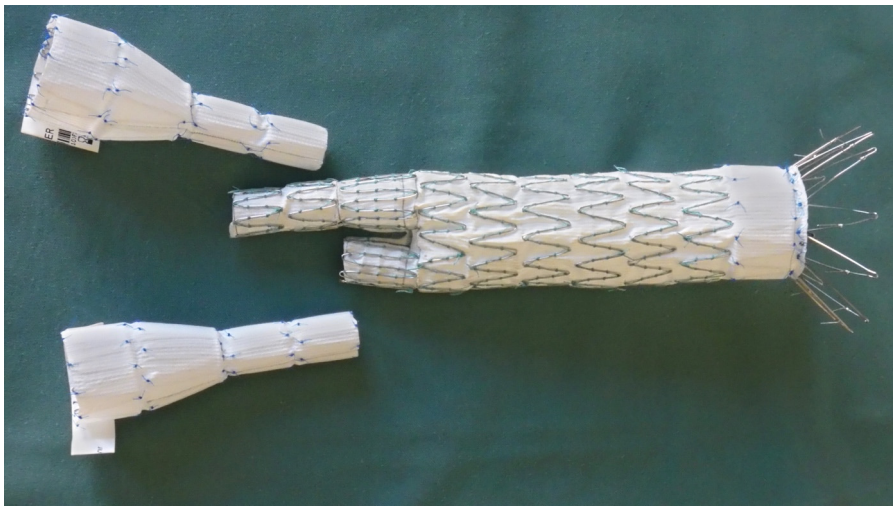

Figure 2.
Standart aortic stentgraft with modular leg.

This standard endovascular aortic treatment method has become popular due to its lower frequency of immediate complications, and its association with shorter in-hospital stay (3, 6, 31). The standard technique is feasible when the distance from the renal and other visceral arteries to the neck of aortic aneurysm is 1.0 cm or more, depending of the angulation of the infrarenal aorta (16, 32). For patients with more complicated aortic anatomy with visceral artery insertions closer to or in the aneurysm sac, new techniques using fenestrated or branched stentgrafts have been developed (33).

Complications

Several studies have proven that endovascular aortic repair is associated with a higher incidence of reinterventions compared to open surgical aneurysm treatment (3, 34). Endoleaks, stentgraft migration, stentgraft kinking, thromboses in the stentgraft, and stentgraft infections are different potential complications after endovascular aortic treatment necessitating regular postoperative follow-up of patients.

Endoleaks

An endoleak is defined as persistent blood flow in the aortic aneurysm outside the stentgraft lumen (35). The incidence of endoleaks during postoperative follow-up after EVAR has been reported to 15%-25% (36). Incomplete sealing of the aneurysm, like in type 1 or type 3 endoleaks causes continuous blood flow to the

aneurysm sac and a remaining rupture risk. Retrograde blood flow to the aneurysm sac from patent lumbar arteries, the inferior mesenteric artery, or other collateral arteries causes type 2 endoleaks. A type 4 endoleak is related to the porosity of the graft fabric with remaining blood passage through the implant. Endotension, or type 5 endoleak is defined as a continuous growth of the aneurysm sac without any apparent endoleak. This can be caused by a slow remaining endoleak not detectable by any radiographic methods, pressure changes in thrombus formation, or by stentgraft infection (36).

Table 2.
Classification of endoleaks.

Type of endoleak	Characteristic
1	Flow into the aneurysm sac due to incomplete sealing. 1a proximal and 1b distal flow.
2	Reversed blood flow into the aneurysm sac from lumbar arteries, assessory renal arteries, or the inferior mesenteric artery.
3	Inadequeate seal within overlap between stentgraft components causing flow into the aneurysm sac.
4	Blood flow through porosity of the stentgraft material.
5	Endotension, expansion of the aneurysm sac without any obvious endoleak origin.

The incidence of type 2 endoleak at one year after EVAR is 18.9%. This figure decreases spontaneously during further follow-up, however, usually by a spontaneous thrombotic process in the lumbar arteries, and the incidence after the second year of follow-up is 10.2% (37). An observed aneurysm sac expansion of ≥ 5 mm during follow-up is considered as an established indication for treatment of type 2 endoleak.

ONYX® embolization

Endovascular embolization is the method of choice for treatment of type 2 endoleak. There are two main possible approaches for embolization: transarterial and translumbar puncture. When using the transarterial approach, the inferior mesenteric artery or the lumbar arteries are selectively catheterized and embolized with small metallic spirals, coils, or a liquid embolic agent like Histoacryl®(n-butyl-2-cyanoacrylate) or Onyx®(tantalum powder and ethylene-vinyl-alcohol copolymer dissolved in dimethyl sulfoxide liquid) (38, 39).

Follow-up after EVAR

Because of the importance of excluding the aneurysm effectively and the continuous pulsation and blood flow in the aorta, the stentgraft and its components can change

their configuration during follow-up after endovascular aortic treatment. It is therefore essential to verify patency of the stentgraft radiologically. Reintervention rate is approximately up to 20% during the first 5 years after intervention (34), corroborating this need for regular radiological follow-up.

Plain radiography

In plain radiography the metallic parts of the stentgraft are clearly visualized, and potential complications such as stent migration, angulation, kink, and breakage can be evaluated. This method can be combined with ultrasound during postoperative follow-up (40).

Ultrasound imaging

The diameter of the aneurysm sac can be assessed with ultrasound and potential endoleak can be visualized with duplex (41-43). With modern ultrasound systems, contrast media based on microbubbles can be used to improve visualisation of blood flow and reveal potential endoleak (42, 44). Important advantages of ultrasound are the absence of radiation exposure and for the fact that no nephrotoxic iodine contrast media is needed. The visual accuracy of the method is poor in obese patients, however, and the method is operator dependent.

Computed tomography angiography

CTA is the method of choice due to its high accuracy for detection of endoleaks, demonstration of aneurysm growth, and potential stentgraft migration (45). Major drawbacks with CTA, on the other hand, are the need for intravenous contrast media and radiation. High flow endoleaks will be detected with arterial phase scans, whereas slow flow endoleaks may need to be visualized with venous phase scans. In case of calcification in the aneurysm sac, the pre contrast media scan is helpful to differentiate this feature from endoleaks.

Magnetic resonance angiography

MRA has a limited use in endoleak detection because of the metal artefacts caused by stentgraft material. Stentgrafts with nitinol are generally more suitable for MRA imaging, whereas those made of stainless steel might cause enormous artefacts (46, 47). In patients treated with nitinol stentgrafts, MRA is at least as sensitive as CTA to reveal endoleaks, and in some cases even better. MRA is also equally reliable as CTA for measurement of aneurysm sac size and stentgraft position (48, 49). Other advantages of MRA are the lack of ionizing radiation radiation, and the reduced dose of nephrotoxic contrast media. Disadvantages of MRA, on the other hand, are the fact that the method is contraindicated in patients with pacemakers or other electronic implants, and the relatively high costs incurred by this method.

Figure 3.
The left panel shows a plain radiography and the right panel a CT angiography image of the same patient undergoing radiological follow-up after EVAR.

Contrast media induced nephropathy

CIN is defined as an absolute (≥0.5 mg/dl) or relative increase (≥25%) in serum creatinine at 48-72 hours after exposure to a contrast agent compared to baseline serum creatinine values, after exclusion of alternative explanations for renal function impairment (9). The increasing number of diagnostic and interventional radiological procedures performed has resulted in an increasing incidence of renal function impairment, and radiographic contrast media have been estimated to be responsible for 11% of cases of hospital-acquired renal insufficiency. Different risk factors for CIN are listed in table 3.

Table 3.
Risk factors for the development of CIN.

Fixed (non-modifiable) risk factors	Modifiable risk factors
Old age	Volume of contrast media
Diabetes mellitus	Hypotension
Pre-existing renal failure	Anemia and blood loss
Avanced congestive heart failure	Dehydration
Low left ventricular ejection fraction	Low serum albumin level (<35g/l)
Acute myocardial infarction	Angiotensin-convertin enzyme inhibitors
Cardiogenic shock	Diuretics
Renal transplantant	Non-steroidal anti-inflammatory drugs
	Nephrotoxic antibiotics
	Intra-aortic balloon pump

A high prevalence of AAA has been established in meta-analyses of patients with coronary heart disease (50-54). Among men undergoing coronary artery bypass or with three vessel disease, the prevalence of AAA has been estimated to be as high as 11.4%. Coronary artery disease can cause congestive heart failure and cardiorenal syndrome, featuring renal function impairment (55). Considering this fact, it is of special importance to minimize iodine contrast media use for repetitive AAA follow-up in patients with coronary heart disease, while maintaining a sufficient diagnostic level.

CT principles

In CT, a rotating x-ray source (x-ray tube) is used to generate images in three dimensions. During scanning the x-ray tube continually rotates around the imaging subject, during which a detector on the opposite side records the beam intensity passing the subject, i.e. how much the subject attenuates the x-rays. The attenuation describes the radiodensity of the object, and is expressed in Hounsfield units (HU) or CT number. During spiral or helical scanning, the subject simultaneously moves perpendicular to the plane of rotation of the x-ray tube and detector.

Dual energy CT

Multidetector CT systems use an array of detector rows, allowing simultaneous acquisition of image data from multiple parallel slices thus reducing examination time. Modern CT systems have 16 to 320 rows or slices. One of the latest technical CT advances is dual energy CT (DECT) or multi energy CT (56-58).

Most of the tissue in the human body consists of atoms like hydrogen, oxygen, carbon, and nitrogen with stable photoelectronic interaction with x-ray beams. Calcium in bone and iodine in intravenous contrast agents have different attenuation properties at different x-ray energies, and this is being utilized in dual or multi energy CT. This capacity allows to highlight or subtract different tissues or structures in the images in dual or multi energy CT (59).

At present, there are several different dual energy CT equipment commercially available. In dual-source CT, two separate x-ray tubes rotate at different voltages with two corresponding detectors. Another diagnostic approach is a rapid voltage switching CT tube with somewhat less hardware requirements. In this model, the tube potential follows a pulsed curve, and acquired photon data is collected twice for every projection. A third diagnostic approach consists of two detector layers with their maximum sensitivity for different photon energies. In a fourth application, two rapid sequential scans with two different tube potentials are used to obtain the

data set (60). As the data is not produced simultaneously, patient motion between the two scans can cause severe degradation of the resultant images. To minimize the time-delay a different approach has been invented, where one axial scan is performed at each tube potential prior to table incrementation.

Novel techniques have been developed for multi-energy data acquisition with energy-resolving photon counting detectors. These semiconducting detectors are capable to count discrete photon interactions by converting the absorbed x-ray energy directly into electrical charge. Improved spectral separation and increased radiation dose efficiency are potential advantages of this technique (60-62).

Radiation dose and image quality

The main disadvantage of CT is the need for use of ionizing radiation, which can cause direct tissue damage or changes in the human genome and increasing risk of carcinogenesis. In CT, the radiation dose is dependent on the same factors as the image quality: tube current (mA), slice scan time (s), and peak tube voltage (kVp) (63).

Before CT came into more popular clinical use, planar radiography and fluoroscopy constituted almost all radiological imaging used. Therefore, it was meaningful to measure the radiation entering to the patient surface (referred to as entrance skin exposure). During CT scanning the x-ray beams reach the patient from all directions, and it is therefore difficult to approximate where in the tissue the maximal radiation dose occurs. This fact has necessitated the development of more reliable radiation exposure measurement methods.

Presently, two standard CT dosimetry phantoms are used to measure CT radiation dose: a 32 cm-diameter cylindric acrylic phantom to represent the body, and a 16cm-diameter version to represent the head. The radiation quantity in spiral CT is the computed tomography dose index by volume ($CTDI_{vol}$), expressed in milligray (mGy). $CTDI_{vol}$ calibrated with CT phantoms is a measure of the radiation output, and not a direct radiation dose measure for a particular patient. Patient dose (mGy) is dependent on $CTDI_{vol,}$ and both patient composition and volume. The total radiation exposure of a CT examination is defined by the dose-length product (DLP = $CTDI_{vol}$ × scan length in centimetres) (64). An estimate of the effective dose expressed in millisievert (mSv) can be obtained by multiplying DLP by a conversion factor appropriate for different anatomical regions. The effective dose reflects the stochastic risk of radiation-induced complications, such as cancer induction.

Image quality in CT, as in all radiography, depends on four fundamental components: image contrast, spatial resolution, image noise, and artefacts.

- Image contrast is determined by an attenuation differential in the image object. In other words, the differences in x-ray attenuation by absorption or scattering in different types of tissue.
- Spatial resolution in CT is the ability to distinguish small, closely spaced objects on an image. This is determined by the distance between the object and the CT detector, focal spot size, detector size, reconstruction matrix resolution, and slice thickness (63).
- Image noise is the fluctuation in CT numbers of homogenous tissue in the CT image, the graininess in the image. This is due to the limited number of photons producing the image. By increasing the tube current, the number of x-ray photons are increased. Scan (rotation) time changes detect x-rays proportionally. Changing the nominal slice thickness changes the beam width entering each detector. Increasing peak tube voltage increases the number of x-rays penetrating the patient and reaching the detectors.
- Image artefacts can be defined as any structure that is seen on an CT image which is not representative of actual patient anatomy. Artefacts can be caused by the patient (e.g. metal and motion artefacts), by radiation physics (e.g. beam hardening, photon starvation, partial volume), or by the CT system (e.g. ring and distortion artefacts) (65).

In clinical CT imaging, the aim is to produce images of diagnostic quality using the lowest possible radiation exposure. This can be summarized with the acronym ALARA,"As Low As Reasonably Achievable" (66).

Image reconstruction

Over the past years, development of the computational capacities of CT systems in clinical use have provided opportunities for both improvements of image quality and simultaneous reductions of radiation doses (67-70). Image reconstructions using different mathematical algorithms play important roles in this process.

Reconstruction algorithms

Filtered backprojection

The CT scanner produces images of different body parts from multiple angles or projections around the body (64). For any given projection there is a line of lighter or darker pixels, i.e. different attenuation depending upon how much of the x-ray beams that passes through the examined body. This pixel volume is called the

projection domain, the raw data of CT numbers, and has sinusoidal undulations as the CT tube rotates around the patient during horizontal movement of the CT table. Such raw CT data with sinusoidal form are also called a sinogram. The standard method of reconstructing CT images is backprojection, in which the CT data is mathematically projected back at the angle from which it was acquired, resulting in an image of this data, also called image domain. This backprojected image is blurry as the image pixels do not appear exactly where they belong. The image domain is therefore mathematically filtered back, resulting in more accurate placement of image pixels and thus a sharper image. This method is called filtered backprojection (FBP) (71).

Iterative reconstruction (IR) methods

When FBP is based on only a single image reconstruction, iterative reconstruction algorithms use multiple repetitions of the image reconstructions for a more accurate result. CT manufacturers have nowadays developed their own specific solutions, offering very little official information on algorithm principles and details (72). IR algorithms can be differentiated in three major subgroups, however: pure iterative methods without any modelling, statistical methods with modelling of the photon counting statistics, and model-based methods which go beyond statistical modelling (73).

- All pure iterative reconstruction methods consist of three major steps which are repeated multiple times until a satisfactory image quality is reached. The first step is a forward projection of the current volumetric image. The second step is comparison of the measured raw data volume. In the third step, this updated image is projected back to the current volumetric image and compared again. These steps are repeated until the current volumetric image reaches a predefined quality criterion.
- Statistical methods incorporate counting of detected photons, and use statistics in the image reconstruction process. Statistical methods can work either in the projection domain or in the image domain.
- Model-based methods attempt to model the acquisition process and use image domains as three-dimensional objects (geometric modelling), or use photon interactions in the addressed object (physical modelling).

Reconstruction of virtual non contrast images

In a DECT system, one scan results in two sets of projection volume where the voxels containing iodine (contrast media) differ from each other. Using mathematical algorithms, iodine can been subtracted from the final image creating a virtual non contrast image (VNC), i.e. an image without contrast material

enhancement of the tissues (60). If the VNC images are of sufficient quality, the true non contrast (TNC) images can be replaced (74). In CT studies after EVAR, this could be helpful to differ an endoleak from the calcium in the aneurysm sac and thereby allow the examiner to omit the TNC scan. This would result in significant radiation dose reduction during repetitive EVAR follow-up CT studies (75).

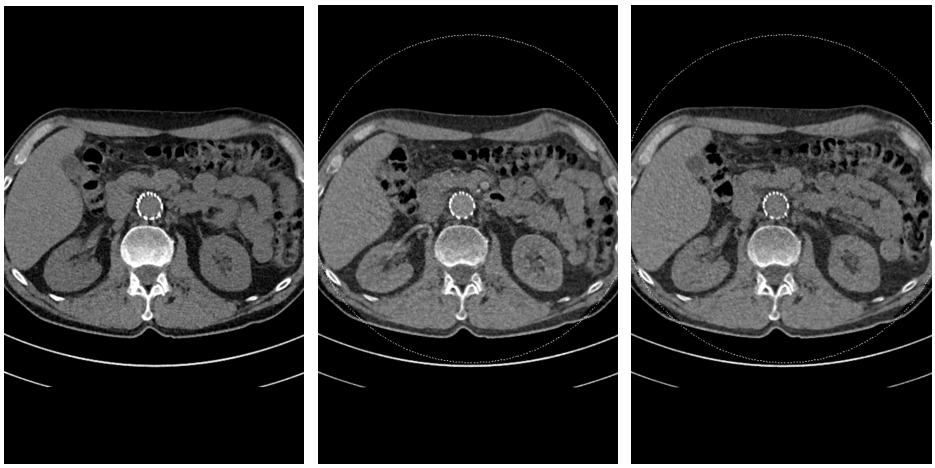

Figure 4.
The left panel shows a TNC image, the middle panel a VNC image derived from an arterial phase scan, and the right panel shows a VNC image derived from a venous phase scan.

Metal artefacts and metal artefact reduction methods

As photons in x-ray beams behave remarkably different in metal objects compared to in human tissue, orthopaedic implant or vessel stents often cause artefacts in the form of streaks, dark shadows, or increased noise. This is due the much higher atomic numbers of metal materials compared to body tissue, and the usually sharply defined borders of medical implants (65). Such phenomena result in decreasing image quality, and causes that important structures like tumours or broken stents can be covered by artefacts. To overcome this problem many different computational methods has been developed. These methods can be roughly divided into the following groups:

- Sinogram inpainting methods, where metal artefact corrupted data is replaced using interpolation.
- Forward projection methods, where metal affected values are treated as missing data (76) and replaced with the value of soft tissue.
- Filtering methods, which try to use all the available information and to not replace metal affected data (77).

- Iterative methods incorporating physics behind the acquisition process, and photon statistics to complete metal affected data (78, 79).

Combined use of several of these artefact reduction methods lead to better image quality and diagnostic certainty (80, 81). In most modern CT systems, several of these methods are combined into an iterative loop for maximal diagnostic benefit (82).

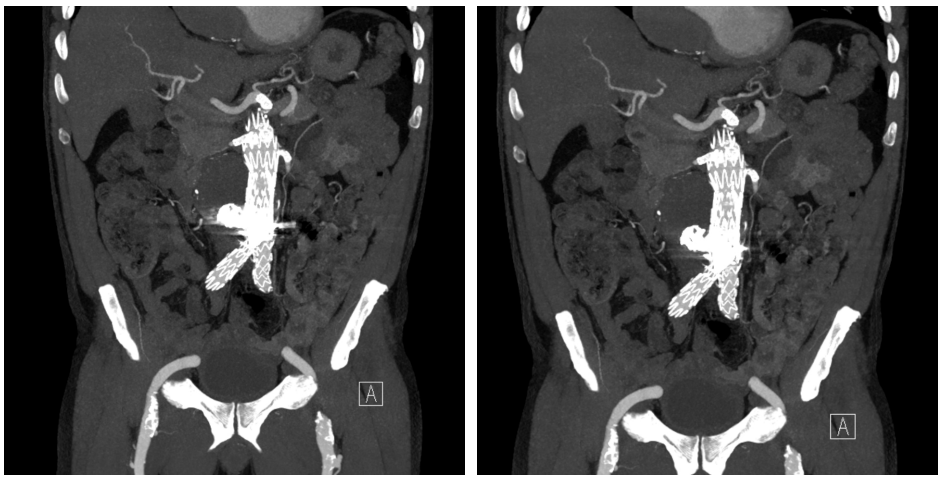

Figure 5.
In the left panel streak artefacts from stent material and Onyx® embolization material is visualized. In the right panel a metal artefact reduction algorithm is used and less streak artefacts therefore appear in the surrounding structures. Images were reconstructed in the CT system Siemens Somatom Definition Flash.

Aims

General aims

The main objectives of this thesis were to assess techniques to improve patient safety, to assess possibilities to reduce radiation dose, and to evaluate possibilities to improve image quality by using metal artefact reduction techniques in CT follow-up after EVAR.

Specific aims

Paper I

- To retrospectively compare vascular attenuation, image noise, image-to-noise ratio, subjective image quality, and radiation effective dose for CTA at 80 kVp after EVAR using a contrast medium dose which is half of that used at 120 kVp.

Paper II

- To compare image quality of virtual non contrast (VNC) images reconstructed from arterial phase dual-energy CTA to true non contrast (TNC) images.
- To assess whether VNC images are of sufficient quality to replace TNC images.

Paper III

- To compare image quality of VNC images reconstructed from arterial and venous phase dual-energy CTA to TNC images.
- To assess which of the above that is most suitable to replace TNC images.

Paper IV

- To evaluate whether post-processing of CT images using metal artefact reduction algorithms can reduce artefacts caused by Onyx® embolization material, and improve diagnostic quality compared to standard image reconstructions.

Material and methods

Patients

Paper I

All patients included in this study were referred for EVAR follow-up by CTA on clinical grounds and were examined as part of a routine program. Two different CT study protocols were used depending on estimated glomerular filtration rate (eGFR); an 80-kVp protocol for those with eGFR < 45 mL/min and a 120-kVp protocol for those with eGFR ≥ 45 mL/min.

Table 4.

Basic characteristics of patients in paper I undergoing 80 and 120 kVp CTA with a 16-multirow detector system for follow-up after EVAR. Median values (2.5 and 97.5 percentiles) presented unless otherwise stated. GFR = glomerular filtration rate, kVp = peak kilovoltage.

Variables	80 kVp cohort	120 kVp cohort
Number of patients	40	40
Men, number (percent)	27 (68)	35 (89)
Age (years)	74 (67-86)	75 (60-82)
Weight (kg)	80 (56-102)	77 (64-110)
Height (cm)	172 (160-183)	177 (160-188)
Body mass index (kg/m^2)	27 (20-35)	24 (19-34)
Plasma creatinine (μmol/L)	139 (76-220)	89 (53-132)
Estimated GFR (mL/min)	38 (22-49)	62 (45-100)

Paper II

Thirty consecutive patients were examined by dual-energy CT and included in the study. Twenty-five patients underwent examination for suspected acute aortic disease and five patients were examined due to a suspected acute complication after abdominal EVAR.

Table 5.
Basic characteristics of the study patients in paper II. Median values (2.5 and 97.5 percentiles) are given unless otherwise stated.

Variables	
Patients (n)	30
Age (years)	65 (37-89)
Weight (kg)	77 (53-126)
Height (cm)	171 (158-193)
Body mass index (kg/m^2)	26 (19-34)
Plasma creatinine (μmol/L)	81 (46-122)

Paper III

Between May 2014 and April 2015, 63 patients (53 men and 10 women) were examined by dual-energy CT for routine follow-up after EVAR, and included in the study. Patients with a body mass index (BMI) > 35 kg/m^2 were excluded because of the presumed insufficient transmission of 80 kVp quanta. Patients with impaired renal function (glomerular filtration rate < 45 ml/min) were examined with a reduced contrast medium dose.

Table 6.
Basic characteristics of the study patients in paper III. Median values (2.5 and 97.5 percentiles) are given unless otherwise stated.

Variables	
Patients (n)	63
Age (years)	73 (63-84)
Weight (kg)	78 (60-106)
Height (cm)	175 (160-186)
Body mass index (kg/m^2)	25 (20-35)
Plasma creatinine (μmol/L)	87 (50-136)

Paper IV

Twelve patients (1 woman and 11 men) referred for follow-up CT angiography after Onyx® embolization for endoleaks following EVAR were recruited for the study between December 2014 and December 2018. Patients with impaired renal function (glomerular filtration rate < 45 ml/min) were excluded. Embolization areas were in the aortic aneurysm sac, the lumbar arteries, the inferior mesenteric artery, and/or in the hypogastric artery aneurysm sac.

Table 7.
Patient characteristics in paper IV (median and range).

Variables	
Patients (n)	12
Age (years)	74 (44-87)
Weight (kg)	86 (60-132)
Height (cm)	177 (160-191)
Body mass index (kg/m^2)	27 (21-41)
Plasma creatinine (μmol/L)	87 (49-110)

Ethical considerations

Paper I was a register study of patients included in the clinical quality assurance program of Skåne University Hospital. No informed consent was therefore required, and the local ethics committee waived ethical approval for publication of the results. The ethical committee of Lund approved the studies reported in papers II, III, and IV (#2014/811).

CT parameters

All the study protocols in papers I-IV were those used for routine clinical studies at Skåne University Hospital. Triphasic (one phase without contrast media, arterial and venous phases with contrast media) study protocols were used except in paper II, in which 25 patients were studied with a diphasic study protocol (one without contrast media and one with arterial phase contrast media) and five patients were studied with a triphasic study protocol. The first study reported in paper I was performed with a 16-row detector CT system, whereas the three following studies (papers II-IV) were carried out with a 128-row, dual-energy CT system.

Table 8.
Sacanning parametres in the studies in contrast phase scan.

	Paper I	Paper II	Paper III	Paper IV
CT system	Siemens Somatom Sensation 16	Siemens Somatom Definition Flash	Siemens Somatom Definition Flash	Siemens Somatom Definition Flash
Source	Single	Dual	Dual	Dual
Tube voltage (kV)	120 or 80	80/Sn140	80/Sn140	80/Sn140
Reference tube load (mAs)	100 or 30	210/81	210/81	210/81
Pitch	1.0 or 0.5	0.85	0.55	0.55
Detector configuration	16 × 0.75/16 × 1.5	128 × 0.6	128 × 0.6	128 × 0.6
Rotation time (s)	0.5	0.33	0.33	0.33
Matrix	512 × 512	512 × 512	512 × 512	512 × 512
Reconstructed slice thickness (mm)	3	5	3	3
Automatic dose modulation	CareDose 4D™	CareDose 4D™	CareDose 4D™	CareDose 4D™
Convolution kernel	B30F	D26f	I30f	I30f

Radiation dose

For all acquisitions, the effective dose was calculated from the dose-length product registered by the CT system, and multiplied by the mean of the conversion factor for abdomen/pelvis in three of the studies (papers I, III, and IV), and for chest/abdomen/pelvis in paper II based on the tissue weighting factors of the International Commission on Radiological Protection 2007 (83). In papers III and IV both the arterial and venous phase scans were performed with dual source system mode, whereas in paper III both contrast media scans were reconstructed and evaluated. In paper IV only arterial phase images were reconstructed and evaluated. In paper IV the radiation parameters were not stated in the ordinary manuscript, as the study aim was to compare standard reconstruction in the arterial phase scan to several reconstructions with metal artefact reduction algorithms produced from already existing arterial phase scans.

Radiation parameters paper I

Table 9.
Radiation parameters in arterial phase scans with 16-slice multirow CT system. Median values (2.5 and 97.5 percentiles) presented unless otherwise stated.

Variable	80 kVp cohort	120 kVp cohort
Scan time (s)	20	20
Scan length (cm)	46 (39-58)	47 (39-53)
$CTDI_{vol}$ (mGy)	7.7 (5.1-9.1)	6.3 (5.0-9.9)
Dose-length product (mGy*cm)	366 (246-459)	320 (207-527)
Effective dose (mSv)	5.1 (3.4-6.4)	4.5 (2.9-7.4)

Radiation parameters paper II

Table 10.
Radiation parameters of true non-contrast (TNC) acquisitions and virtual non-contrast (VNC) acquisitions. Median values (2.5 and 97.5 percentiles) presented unless otherwise stated.

Variables	TNC	VNC
Scan time (s)	6 (5-7)	4 (4-7)
Scan length (cm)	67 (55-77)	64 (55-73)
$CTDI_{vol}$ (mGy)	7.2 (4.3-11.3)	6.5 (5.6-9.6)
Dose-length product (mGy*cm)	492 (262-875)	460 (380-760)
Effective dose (mSv)	9.0 (4.8-16.1)	8.4 (7.0-13.9)

Radiation parameters paper III

Table 11.

Radiation parameters of true non-contrast (TNC) acquisition and virtual non-contrast arterial phase (A-VNC) and venous phase (V-VNC) reconstructions. Median values (2.5 and 97.5 percentiles) are given unless otherwise stated. $CTDI_{vol}$, volume computed tomographic dose index; mGy, milliGray; mSv, milliSievert.

Variables	TNC	A-VNC	V-VNC
Scan time (s)	7 (6-8)	7 (6-8)	7 (7-8)
Scan length (cm)	48 (41-54)	48 (41-54)	48 (41-54)
$CTDI_{vol}$ (mGy)	5.1 (3.6-7.9)	4.9 (3.4-8.4)	4.9 (3.4-8.4)
Dose-length product (mGy*cm)	267 (166-403)	269 (171-429)	257 (162-420)
Effective dose (mSv)	3.7 (2.3-5.6)	3.6 (2.3-5.9)	3.6 (2.3-5.9)

Radiation parameters paper IV

Table 12.

Radiation parameters of arterial phase contrast acquisitions. Median values (minimum and maximum) are given unless otherwise stated.

Variables	Arterial contrast phase acquisition
Scan time (s)	7 (7-12)
Scan length (cm)	50 (43-75)
$CTDI_{vol}$ (mGy)	6.0 (3.7-9.6)
Dose-length product (mGy*cm)	335 (165-600)
Effective dose (mSv)	5.2 (2.6-9.2)

Image reconstructions

In paper I, arterial phase 3 mm thick axial images were reconstructed automatically by the CT system for both the 80 kVp and 120 kVp patient cohorts. In paper II the 5 mm thick axial TNC images were automatically reconstructed by the dual-energy CT system, whereas Siemens Syngo.via software was used in the radiological workstation to reconstruct the 5 mm thick axial VNC images. For TNC images, the iterative reconstruction algorithm SAFIRE was used at level one. In papers III and IV, true non contrast (TNC) axial images and standard arterial phase axial images were automatically produced by the CT system. Virtual non-contrast (VNC) axial images and images with different Siemens metal artefact reduction algorithms (iMAR) were reconstructed at the workstation of the CT system.

Table 13.
Overview of the image reconstruction process in papers I-IV. VNC = virtual non-contrast, A-VNC = VNC image from arteral phase acqistion, V-VNC = VNC image from venous phase acquisition. MAR = metal artefact reducing algorithm.

	Paper I	Paper II	Paper III	Paper IV
Reconstruction system	Siemens Sensation 16, consol	Siemens Syngo.via software	Siemens Definition Flash, consol	Siemens Definition Flash, consol
Slice thickness	3	5	3	3
Iterative algoritms	-	SAFIRE®, level 1	SAFIRE®, level 1	SAFIRE®, level 1
VNC	-	A-VNC	A-VNC, V-VNC	-
MAR	-	-	-	8 different variants

Image quality assessment

The image quality was evaluated with both objective measurements (papers I-IV), and subjective assessment (papers I, II, and IV). The radiological PACS workstation (IDS7, Sectra Imtec AB, Linköping, Sweden) was used to measure mean attenuation values (HU) and noise (standard deviation, HU) in the images (papers I-IV). Mean attenuation values and image noise were measured in the aorta at the levels of the hemidiaphragms, the renal arteries, and the aortic bifurcation (papers I- II). Identical mean vascular attenuation were measured at the levels of the hemidiaphragms, the renal arteries, the right lobe of the liver, the retroperitoneal fat, and the psoas muscle (paper III), or at the aorta at the level of the hemidiaphragms, and the aorta or iliac arteries close to the Onyx® embolization material (paper IV). The regions of interest (ROI) in the arteries were made as large as possible while avoiding calcifications, plaques, and stent material. In paper I, contrast-to-noise ratio (CNR) was calculated to evaluate the sensitivity to detect potential endoleak in the aneurysm sac and thrombus.

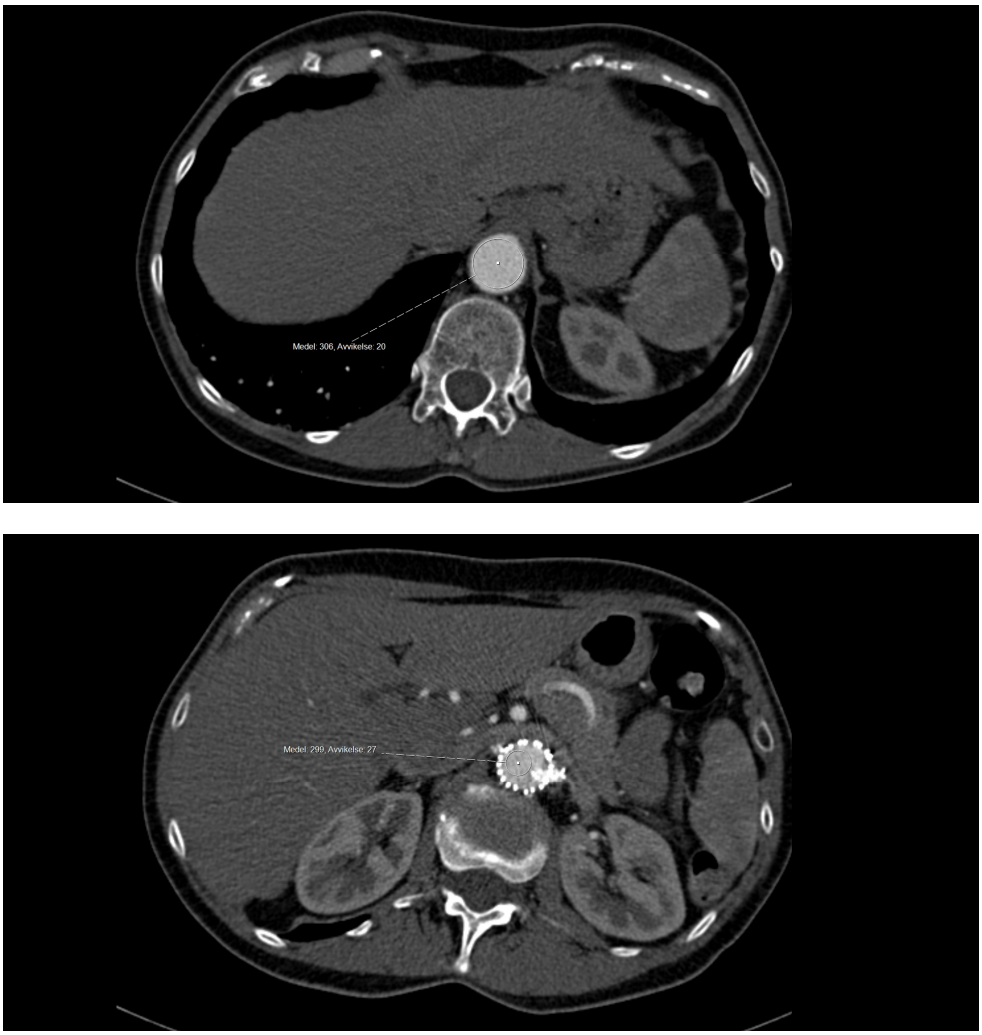

Figure 6.
The upper panel shows the ROI in the aorta at the level of diaphragm, and the lower panel shows the ROI in aorta in the level of renal arteries. The maximum diameter of the ROI is measured avoiding contact with the stent.

Table 14.
Overview of objective and subjective image quality assessment methods used in the different studies.

Method	Paper I	Paper II	Paper III	Paper IV
Objective methods				
CT numbers (HU)	x	x	x	x
Noise (HU)	x	x	x	x
Contrast-to-noise ratio	x			
Subjective method				
Overall image quality	x	x		x
Feasibility to detect vessel patency				x
Assessment of artefacts		x		x
Feasibility to detect endoleaks	x			x
Residual contrast (VNC)		x		
Subtracted calc		x		
Subtracted stents		x		
Ability to see adjacent structures close to Onyx®				x
Inter-observer agreement	x	x		x

Subjective evaluation was performed independently and blinded by using ViewDEX, a computer software developed for randomized analysis of digital images (84, 85). Assessments were made by two radiologists in papers I, II, and IV, and by one radiologist and one vascular surgeon in paper I. A four-point scale was used (4 = excellent; 3 = good; 2 = moderate quality but sufficient for diagnosis; 1 = non-diagnostic) with more specific criteria for each point assessed.

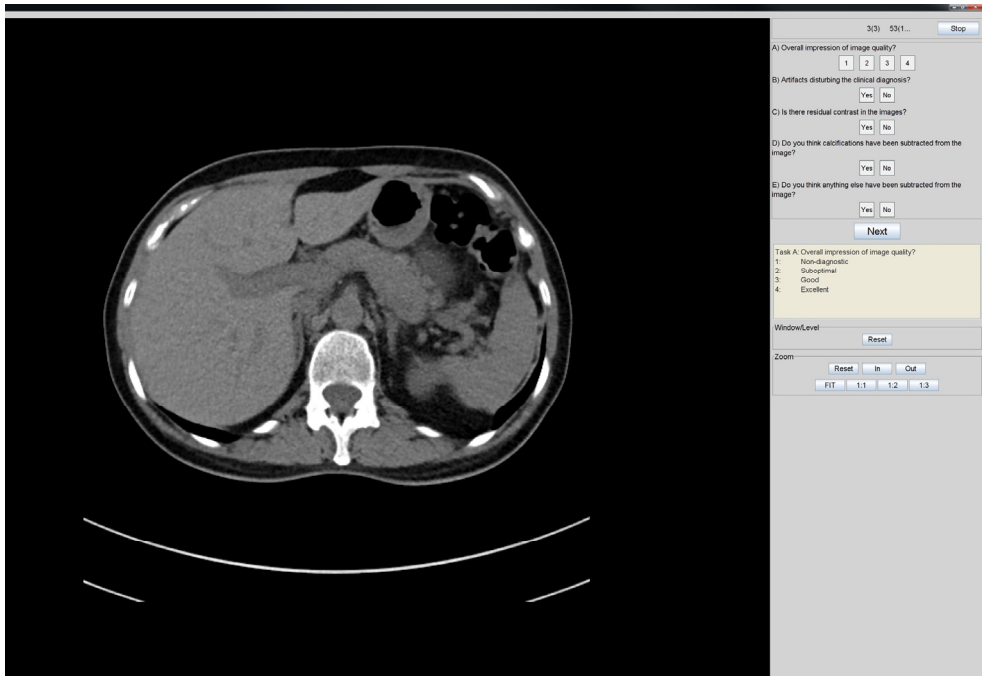

Figure 7.
Picture showing the ViewDEX layout in a PACS workstation.

Statistical evaluation

Statistical analysis was performed using the statistical software SPSS (version 24.0-25.0; SPSS Inc, Chicago, IL, USA).

In paper I the Mann-Whitney U-test was used to compare differences between the two cohorts regarding the ratio used gram iodine/GFR, scan time and length, vascular attenuation, thrombus attenuation, noise, CNR, radiation doses, and subjective evaluation of image quality. A p-value < 0.05 was considered significant.

In paper II the Mann-Whitney U-test was used to compare differences between the TNC and VNC datasets regarding vascular attenuation, noise, and radiation dose. Wilcoxon´s signed-rank test was used to compare the subjective evaluations of image quality. In both tests a p-value < 0.05 was considered significant. Inter-observer agreement regarding overall image quality was assessed using the intra-class correlation coefficient (ICC).

In paper III median, minimum and maximum were used to describe the distribution of attenuation and noise differences, and the Wilcoxon's signed-rank test was used

to determine differences between the TNC and VNC datasets. A p-value < 0.05 was considered significant.

In paper IV median, minimum and maximum were used to describe the distribution of attenuation and noise differences. The Wilcoxon signed-rank test for paired samples was used to assess statistical significances and to compare outcomes of the subjective evaluation of image quality. The level of significance was set to $p < 0.05$.

Results

Paper I

Aortic attenuation using the 80-kVp protocol with halved contrast media dose was not inferior compared to the 120-kVp protocol. With both protocols only a weak correlation between mean aortic attenuation and body weight was demonstrated, as could be expected with the used contrast medium injection protocol, i.e. tailoring contrast media dose to body weight and using a fixed injection time.

The only statistically significant differences between the two protocols were higher aortic attenuation at the level of the renal arteries, higher image noise, and higher $CTDI_{vol}$ in the 80-kVp cohort. However, this did not result in any statistically significant differences in aortic CNR, DLP, or effective dose between the 80-kVp and 120-kVp cohorts.

Image noise in the aneurysm thrombus was higher using the 80-kVp protocol compared with the 120-kVp protocol. Despite the differences in image noise between these two protocols, however, there was no statistically significant difference in median aortic CNR. Nevertheless, CNR showed a clear negative correlation with increasing body weight, which is shown in table 3 in the original article.

Correlations between aortic mean attenuation and body weight, and between aortic CNR and body weight are illustrated in Fig. 8.

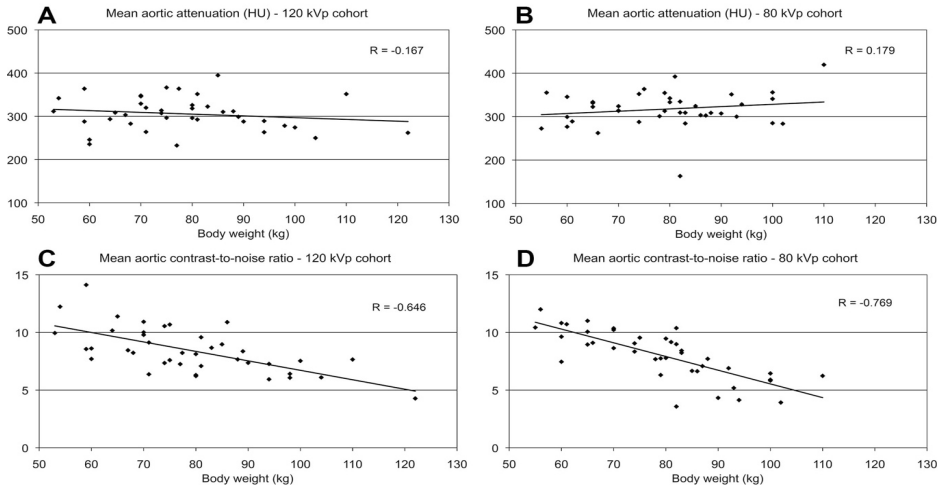

Figure 8.
Aortic attenuation (mean values at the level of the renal arteries and the aortic bifurcation) measured in Hounsfield units (HU) at 120 kVp (A) and 80 kVp (B), and aortic contrast-to-noise ratio at 120 kVp (C) and 80 kVp (D) following contrast medium injection in early arterial phase. r = Pearson correlation coefficient, r^2 = determination coefficient.

The mean overall quality scores in the 80 and 120 cohorts were 3.0 and 3.5, respectively, for reader # 1, and 3.0 and 3.3, respectively, for reader # 2. Overall image quality ($p= 0.003$) as well as image quality at the aortic bifurcation ($p = 0.002$) were significantly better in the 120 than the 80-kVp cohort for reader # 1 , but no difference was seen at the diaphragmatic level ($p = 0.084$). For reader # 2 there were no significant differences in image quality between the two protocols, overall ($p = 0.11$) or at any specific level ($p > 0.23$).

In the 120-kVp cohort no examination was rated as poor concerning overall quality or quality at any of the individual vascular segments. In the 80-kVp cohort one examination was rated as poor concerning overall image quality by one reader and as of moderate quality by the other reader. Both readers rated the examination as being of poor quality at the level of the aortic bifurcation. This examination was performed on a patient with BMI of 37 kg/m^2 (body weight 94 kg), had the highest image noise (82 HU), and an aortic CNR of 4.1. One reader rated another 80-kVp examination as being of poor quality at the level of the renal arteries, whereas the other reader rated it as being of moderate quality. CNR was 2.8 and the only aortic mean attenuation < 200 HU (159 HU). The iliac arteries could be assessed in all patients.

Paper II

At all aortic levels the VNC images had significant higher attenuation ($p < 0.001$) and image noise ($p < 0.001$). This is shown in table 4 in the original article.

When comparing the VNC images to the TNC images, side-by-side artefacts in major thoracic vessels could be demonstrated in VNC images (Fig 9, pulsation). Removal of minor arterial calcifications occurred in 22 out of 30 VNC images. In all cases, these removed calcifications were small, 1-3 mm, and located at the aortic or iliac wall (Fig 9, calcification). Partial removal of stent structures occurred in the VNC images of two patients, one stent was partially subtracted from the left renal artery, and in another case an aortic stent was partially subtracted (Fig 9, stent). In five cases, significant noise was demonstrated in the VNC images (Fig 9, noise). These patients had BMI of 26, 24, 33, 26, and 33 kg/m^2, respectively, three were women and two were men. One of these five patients had undergone fenestrated EVAR, and four had been referred to the study because of suspected aortic rupture.

In subjective image quality evaluation, all TNC images were rated as being of good or excellent quality. The mean image quality scores were 3.6 for reader # 1 and 3.7 for reader # 2. All VNC images were rated as being of moderate to excellent quality, with a mean image quality score of 3.0 for reader # 1 and 3.2 for reader # 2. There was a significant ($p < 0.001$) difference in subjective image quality between the TNC and VNC datasets. For the overall image quality, the inter-observer agreement was moderate with average ICC value of 0.743.

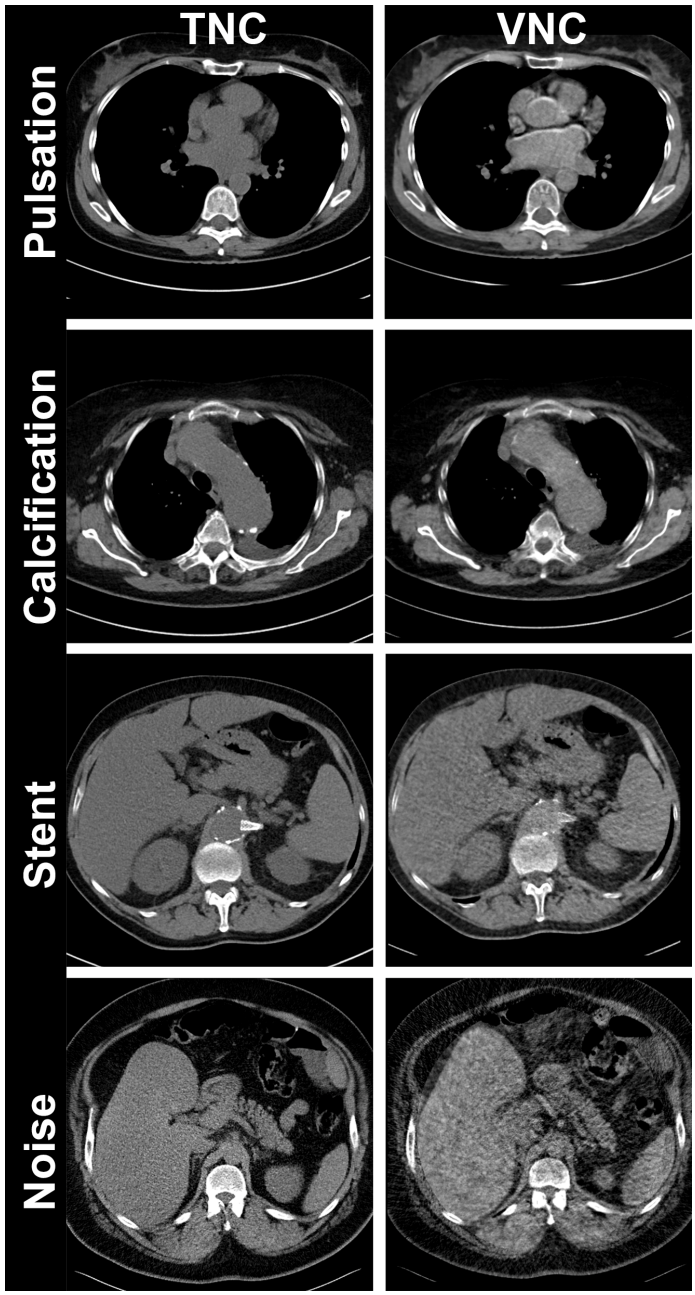

Figure 9.
Artefacts in the VNC images.Pulsation: Attenuation artefacts in main thoracic vessels in the VNC image. Calcification: Elimination of the small calcifications in the aortic wall in the TNC image. Stent: A partly removed renal stent. Noise: Incomplete elimination of the contrast media in the VNC image on the right in the abdominal aorta.

Paper III

This prospective study showed that in terms of aortic attenuation values, VNC images reconstructed from venous phase CT angiography (V-VNC) represent a better approximation of TNC images than those reconstructed from arterial phase (A-VNC) scans. Attenuation differences were significant between the TNC and both the VNC images at the level of the diaphragmatic aorta, whereas there were no significant difference between TNC images and V-VNC images at the level of the renal arteries. In both VNC images, the attenuation values in liver and fat tissue were significantly higher compared to TNC images. In muscle (psoas) tissue, attenuation values were higher in A-VNC images compared to TNC images, whereas no significant differences were demonstrated between V-VNC and TNC images. Neither were there any significant differences in image noise between the TNC and both the VNC images. Differences in attenuation values and image noise are presented in Table 17.

Table 17.

Differences in attenuation (HU) and image noise (1 SD, HU) between the true non-contrast (TNC) acquisition and the virtual non-contrast images acquired from arterial (A-VNC) and venous phase acquisition (V-VNC) at the levels of the diaphragma and the renal arteries. Statistical significance (p-values) between differences in attenuation was calculated using Wilcoxon Signed Rank test.

Anatomic position	Δ A-VNC - TNC	Δ V-VNC - TNC	Δ A-VNC - V-VNC
Aorta at diaphragmatic level			
Attenuation (HU)	44 ($p < 0.001$)	8 ($p < 0.001$)	36 ($p < 0.001$)
Image noise (HU)	3	2	1
Aorta at renal artery level			
Attenuation (HU)	32 ($p < 0.001$)	3 ($p = 0.13$)	35 ($p < 0.001$)
Image noise (HU)	1	2	3

Paper IV

In all iterative MAR (iMAR) reconstructions the differences in attenuation between the reference level (diaphragmatic aorta) and the vessel lumen affected by metal artefacts were significantly smaller than in the standard images. The same finding could be demonstrated for psoas muscle. The study showed that iMAR reconstructions constitute better representation of vessels and muscles than standard images of areas affected by metal artefacts from Onyx®.

The smallest attenuation differences, i.e. the most accurate representation, were seen in reconstructions tailored for *Pacemaker*, *Shoulder implants,* and *Dental fillings*, as shown in Table 18. Attenuation reduction was significantly different between the standard image and iMAR reconstructions for *Neuro coils* ($p = 0.005$), *Shoulder*

implants (p = 0.006), *Pacemaker* (p = 0.015), *Thoracic coils* (p = 0.006), *Hip implants* (p = 0.021), and *Extremity implants* (p = 0.019). The smallest attenuation differences between the reference ROI in the psoas muscle at the level of the diaphragm compared to the ROI at the level of the Onyx® were seen in iMAR reconstructions tailored for *Spine implants, Shoulder implants, and Thoracic coils.*

Table 18.

Attenuation differences between artefact-affected and non-affected vessel lumen and psoas muscle. Median and range for attenuation (HU) and noise (SD) differences for vessel lumen and psoas muscle at the level of Onyx®, compared to reference levels.

	△ HU/SD aorta/artery		**△HU/SD psoas diaph/Onyx**	
Reconstruction	**△ HU**	**△ SD**	**△ HU**	**△ SD**
Standard	232 (46-707)	62 (13-99)	17 (6-109)	15 (2-115)
Neuro coils	151 (43-475)	79 (7-172)	16 (1-27)	4 (0-83)
Dental fillings	122 (21-306)	82 (7-264)	15 (2-30)	9 (1-107)
Spine implants	191 (52-598)	39 (3-157)	12 (6-27)	12 (1-77)
Shoulder implants	119 (47-554)	89 (3-145)	13 (3-27)	6 (0-26)
Pacemaker	112 (24-437)	68 (1-161)	14 (6-26)	6 (1-29)
Thoracic coils	140 (39-377)	74 (13-122)	13 (1-27)	5 (1-29)
Hip implants	137 (1-368)	70 (12-147)	16 (5-30)	6 (0-27)
Extremity implants	127 (17-443)	65 (8-186)	15 (5-36)	5 (2-28)

The iMAR reconstructions were all rated with higher scores by both readers for overall image quality compared to the standard images. The standard images were generally rated as non-diagnostic or acceptable, whereas images reconstructed with iMAR algorithms were rated as acceptable or good. The most prominent difference in subjective overall image quality as judged by both readers, was seen for iMAR reconstructions tailored for *Hip implants* and *Extremity implant*s compared to the standard images.

Discussion

Potential complications occurring after EVAR mandate regular follow-up examinations with CT angiography, but these patients may have several important risk factors for contrast media induced renal function impairment. Therefore, attempts to individually optimize contrast media and reduce radiation dose in CT angiography are highly desirable.

In CT angiography both timing and concentration of the intravenous contrast media infusion are crucial to enable diagnostic coverage of the anatomic vascular area of relevance. When decreasing the contrast media dose, the imaging time needed for optimal coverage of the area of interest becomes limited. When decreasing the tube voltage, the image noise increases. These facts are both of clinical relevance when planning the optimal quality in CT angiography. In CT angiography, the contrast agent usually infused in the upper extremities passes fast through the right heart before entering to the pulmonary tree. To cover the abdominal aorta, contrast media has to pass also the left heart, creating a delay which is variable and related to the cardiac output of the individual patient (86). Several previous studies in pulmonary (87-90) or abdominal CT angiography (91) show how the contrast media dose can be reduced through reduction of tube voltage with preserved diagnostic quality. These previously published results gave us reason to believe that this technique would potentially be adequate also in patients treated with EVAR, and served as a basis for paper I. The results of this study have subsequently been introduced in more general clinical use, and have even been included in commercial recommendations (92).

Using the widely accepted tri-phasic CT study protocol repetitively after EVAR results in a substantial radiation dose. By eliminating the first scan without intravenous contrast media, and thus significantly reducing the radiation dose, seemed attractive in the CT follow-up study.

The basic principles for creation of VNC images are widely known, but each CT system manufacturer has its own commercially protected methods to construct VNC images. Applying these methods in a clinical environment is always somewhat dubious. Several previous studies (74, 75) had shown promising results using the VNC technique, and gave us the basic ideas behind papers II and III. The results showing high aortic attenuation values and high noise in VNC images compared to TNC images in paper II were a disappointment, however. This prompted a more

detailed study set up in paper III, using VNC derivatives both from arterial and venous phase scans.

There are some important technical differences to take into account when comparing these two studies. In paper II we used a CT angiography protocol for imaging the entire aorta, whereas in the subsequent paper III a CT protocol aimed for the abdominal aorta was utilized. For paper II, VNC images were reconstructed at a PACS workstation using Syngo.via software (MMWP, version 20; Siemens Healthineers, Forchheim, Germany), whereas the images in paper III were reconstructed at the workstation of the CT system (Somatom Definition Flash, Syngo). Furthermore, convolution kernel D26f was used in paper II and I30f in paper III. The use of iterative reconstruction kernel I30f in paper III can partly explain the differences in noise values in these two studies. In paper II image noise was remarkably higher compared to in paper III, in which image noise was equal to that recorded in TNC images. It might therefore be questioned whether the quality of the available raw CT data is more superior at the CT system compared to the CT image reconstruction performed in the PACS workstation with Syngo.via software. The latter study showed that VNC images derived from venous phase scans constitute a more acceptable substitute for TNC images than images from arterial scans.

As paper III was focused upon evaluation of attenuation values and image noise in VNC images, no subjective image evaluation was performed.

In paper IV we approached the clinically important problem of using highly x-ray positive vessel glue Onyx® to embolize type 2 endoleak after EVAR. Metal artefact reducing algorithms are mathematically very complex and demand high computation capacity, and each CT system manufacturer have therefore developed their own commercially protected algorithms. How these algorithms can be optimally applied in clinical use is a highly relevant question. As these algorithms are optimized to be suitable for most of the currently used medical implants (93-95) made of metals with lower atomic numbers compared to the tantalum in Onyx®, they may not always be effective enough to get rid of the artefacts caused by this agent. The results of this study are comforting, however, as they showed that iMAR might help making the nearly useless standard CT angiography acceptable for diagnosis.

The patient material in paper IV was small, mostly due to the fact that only few patients in the follow-up program at our hospital undergo embolization with Onyx® after EVAR treatment. Paper IV was planned as a pilot study, which might give valuable information for planning a future study project with the purpose to evaluate more metal artefact reducing algorithms in detail in a larger patient material.

Efficient and reliable methods for subjective image quality evaluation enabling true blinding and randomization of images are essential for research. ViewDEX is free to use for non-commercial purposes, and is applicable in a normal radiological workstation. This method was used in papers I, II, and IV for subjective image evaluation. In papers II and II, the use of this software was fluent and rendered reliable pictures for adequate evaluation of the vascular structures of interest. In paper IV on the other hand, this software suffered from several interruptions during image assessment, making subjective image evaluation less optimal than in the previous studies. This fact might partly explain the relatively low inter-observer correlation in this study.

Clinical impact

All the study projects included in this thesis have been conducted in a clinical radiology department. The insights gained from the study reported in paper I have already been translated into clinical routine. We now have two different CT study protocols for EVAR follow-up; one for patients with normal renal function and another for patients with impaired renal function.

Although the results presented in papers II and III were somewhat disappointing, they elucidated the possibility to individually adjust the CT angiography protocol when repeated CT studies are performed in younger patients, and reduction of the radiation dose is highly desirable. Future research with more effective reconstruction algorithms will hopefully demonstrate that VNC images can be an acceptable replacement for TNC images, helping us to significantly further reduce the radiation dose in CT angiography.

Metal artefact reducing algorithms are available in almost all modern CT systems, allowing transformation of non-diagnostic CT studies into diagnostic studies in crucial cases. These algorithms have already been introduced into clinical practise in orthopaedic CT studies, and are currently under evaluation for use in vascular CT studies after EVAR.

Future perspectives

DECT provides another method to differentiate endoleaks from aneurysm sac calcification using the hard plaque imaging algorithm. This can provide a possibility for replacement of TNC scans, and thus for significant reduction of radiation dose in vascular follow-up CT studies. This method seems to be interesting for future studies.

The new metal artefact reducing algorithms were demonstrated to provide an important clinical impact in paper IV, inspiring us to plan a new study in patients operated with more complex EVAR techniques and therefore harbouring a larger number of metallic stent structures. To study image quality comparing iMAR and virtual monoenergetic images with different dual-energy weighting would give us more valuable information for our future clinical radiology practice.

Photon counting detectors will probably also help us to overcome the challenges with metal artefacts when they become more available in clinical use (62). These novel detectors can contribute more effectively to material differentiation, and only one CT acquisition might be needed to visualize calcifications or iodine contrast in the aneurysm sac. This would result in a significant reduction in radiation dose during repetitive CT follow-up after EVAR.

Converting the imaging follow-up after EVAR from CT to contrast-enhanced ultrasound is one of the most efficient ways to reduce radiation dose and the amount of CT studies needed (44, 96). After more complex endovascular aortic repair the stent configuration details may not be revealed accurately enough with this technique, however, and it should therefore be completed with plain radiographs. Only patients with changes in aneurysm diameter or endoleak detected by the ultrasound studies might be subjected to a subsequent CT study. This type of ultrasound based follow-up protocols are already used in clinical practise (97, 98).

Conclusions

New CT techniques and image reconstruction methods can improve patient safety and reduce radiation dose with maintained or even improved image quality.

Paper I

In follow-up CTA after EVAR in patients with impaired renal function, the use of an 80-kVp technique combined with a halved dose of CM tailored to body weight decreases the risk of CIN while preserving diagnostic quality. Presently used CT equipment limits the use of this method in patients with high body weight or obesity, however, and the upper limit seems to be about 90 kg or a BMI of 35 kg/m^2 according to our experience.

Paper II

CT angiography images reconstructed with VNC technique based on arterial phase scan have significantly higher mean attenuation and higher noise levels compared to TNC CT images. Therefore, VNC images derived from arterial phase scan cannot be considered as suitable replacement for TNC images.

Paper III

VNC images based on venous phase scans appear to be a more accurate representation of true non-contrast scans than VNC images based on arterial phase scans, with similar attenuation and noise levels in the aorta compared with TNC scans.

Paper IV

The metal artefact reduction algorithm iMAR can reduce severe metal artefacts in CT angiography after EVAR and following Onyx® embolization, and thereby significantly improve both image quality and diagnostic accuracy.

Populärvetenskaplig sammanfattning

Stora kroppspulsådern är den huvudväg som syrerikt blod tar från hjärtat vidare ut till kroppens alla organ. Av olika skäl kan kroppspulsåders vägg bli svag och tänjas ut, vilket benämns ett pulsåderbråck. Risken för pulsåderbråck är högre hos individer med åderförfettning eller högt blodtryck och för rökare. Risken stiger med åldern och män drabbas oftare än kvinnor. Ofta bildas bråck helt utan symptom och upptäcks inte förrän bråcket spricker. Då detta sker, dör nästan 50 % av patienterna innan de kommer till sjukhuset. Därför kontrolleras stora kroppspulsådern hos alla 65 åriga män i Sverige med ultraljud, så kallad screening. Ibland kan bråcket hittas av en slump, då ofta i samband med röntgenundersökning av en annan sjukdom.

Endovaskulär behandling av kroppspulsåderbråck

Man kan behandla bråck som upptäcks i tid. Då förstärker man kroppspulsåderns vägg med en metallförstärkt kärlprotes. Läkaren gör en liten öppning i ljumsken och för in protesen genom lårpulsådern. Tekniken kallas endovaskulär behandling, vilket betyder att man helt arbetar från blodkärlens insida. Det behövs minst tre kärlproteser som överlappar varandra. Man för in dem en och en, och sätter ihop dem när de är på plats inne i kroppen.

Med denna metod slipper man öppna hela buken och därför är operationen mindre påfrestande för patienten. Den endovaskulära metoden minskar även smärta och behov av intensivvård direkt efter operationen. Många patienter går hem redan två till tre dagar efter operationen. Efter öppen kirurgi tar det mer än dubbelt så lång tid.

Nackdelen med den endovaskulära behandlingen är att patienter ganska ofta får komplikationer, antingen direkt efter operationen eller med tiden. Därför behövs regelbunden kontroll av att kärlproteserna är hela och sitter rätt. Man behöver också se att blodet flyter som det ska genom proteserna.

Uppföljning efter endovaskulär behandling

Den mest tillförlitliga kontrollmetoden är en kontrastförstärkt skiktröntgen som kan avslöja både kärlprotesens läge och blodflödet in i denna. För att visa blodflödet använder man kontrastmedel. Det skadar njurarna, framför allt om patientens njurar redan fungerar dåligt.

Vid skiktröntgen används även joniserande strålning. Upprepade undersökningar kan därför öka risken att få strålningsrelaterad cancer.

Både kärlproteserna och en ”tätningsmassa” som ibland behöver användas innehåller metall. Detta ger allvarliga störningar i skiktröntgenbilder och därmed blir diagnoserna mycket mer osäkra.

Denna avhandling innehåller fyra delstudier. Den undersöker olika tekniska möjligheter att förbättra uppföljningen med skiktröntgen efter behandling av endovaskulärt kroppspulsåderbråck.

Studie I

Man kan göra skiktröntgen med olika inställningar i maskinen. Ofta använder man hög rörspänning därför att det ger allmänt bättre bildkvalitet. Nackdelen är att kontrastmedlet fungerar sämre, så att blod och blodkärl inte syns lika bra. Därför använder man normalt mer kontrastmedel.

Studien jämförde två alternativ med varandra:

- Skiktröntgen med normal kontrastdos och 120 kVp rörspänning hos njurfriska patienter.
- Skiktröntgen med halverad kontrasdos och 80 kVp rörspänning (där kontrastmedlet är mer effektivt) hos njursjuka patienter.

Studien visade att dessa två alternativ var jämförbara, men 80 kVp-tekniken gav inte tillfredsställande kvalitet hos kraftigt överviktiga patienter.

Studie II

Patienter som har endovaskulär kärlprotes behöver uppföljning med skiktröntgen. Den rekommenderade metoden är att utföra undersökningen både utan kontrastförstärkning och med kontrastförstärkning i två omgångar.

Syftet med den här studien var att undersöka om stråldosen kan minskas om man ersätter omkörningen utan kontrast med konstgjorda icke-kontrastförstärkta bilder. En modern skiktröntgenmaskin med två röntgenrör kan återskapa icke-kontrastbilder ur de kontrastförstärkta bilderna.

Studien visade att de återskapade bilderna var av sämre kvalitet än de äkta icke-kontrastförstärkta bilderna.

Studie III

Man kan återskapa icke-kontrastförstärkta bilder på två sätt. Antingen använder man den första körningen, när kontrastmedlet är i artärerna, eller den andra körningen, när kontrastmedlet hunnit till venerna.

Syftet med den här studien var att undersöka om någon av dessa återskapade bilder kan ersätta undersökningen utan kontrast. Resultatet visade att bilderna från den andra omkörningen var jämförbara och därför skulle kunna användas som ersättning. Därmed kan man minska röntgenstråldosen i den enskilda undersökningen.

Studie IV

Syftet var att utvärdera om en ny rekonstruktionsteknik vid skiktröntgen kan minska förekomsten av allvarliga bildstörningar hos patienter som har behandlats med ”tätningsmassa”. Studien visade att störningarna minskade och att undersökningen gav en säkrare diagnos.

Suomenkielinen tiivistelmä

Ihmisen suurin valtimo, aortta, vastaa hyvin hapettuneen veren jakelusta kaikkiin ihmiselimiin. Veren korkeat rasvapitoisuudet, verenpainetauti, tupakointi, korkea ikä ja miessukupuoli lisäävät riskiä aortan seinämän valtimonkovettumatautiin. Tämä tauti voi johtaa vähitellen seinämän haurastumiseen ja aortan laajentumiseen, mikä tapahtuu tavallisimmin vatsan alueella. Yleensä taudin kulku on oireeton ja etenee, kunnes heikentynyt verisuonen seinämä repeää. Koska kyseessä on ihmisen valtasuoni, on tilanne huomattavan vakava: yli 50 % aortan repeytymisissä potilaat kuolevat ennen kuin ehtivät sairaalaan. Tämän vuoksi monissa maissa, kuten Ruotsissa, on kehitetty kansallisia seulontaohjelmia laajentuneen vatsa-aortan havaitsemiseksi. Toisinaan laajentunut vatsa-aortta voidaan havaita jonkun toisen röntgentutkimuksen ohessa ja tällöin se voidaan korjata leikkaamalla ennen vakavaa repeytymistä.

Suonensisäinen aortanpullistuman hoito

Laajentunut aortta voidaan vahvistaa suonensisäisellä proteesilla, joka tuodaan ylös vatsa-aorttaan nivusvaltimon kautta. Suonensisäisiä verisuoniproteeseja todellisuudessa tarvitaan vähintään kolme, jotka sijoitetaan valtimoihin osin limittäin. Tällä tekniikalla vältetään koko vatsan kattavaa leikkaushaavaa, joka on tarpeellista tehdä, jos vatsa-aortta korjataan avoimella leikkaustekniikalla. Suonensisäisen aorttaleikkauksen jälkeinen kipu on vähäisempää ja yleinen toipuminen on huomattavan paljon nopeampaa. Lisäksi tehohoidon tarve leikkauksen jälkeen on merkittävästi vähäisempää. Huonona puolena suonensisäisessä hoidossa on suhteellisen suuri määrä jälkikomplikaatiota sekä lyhyellä että pitkällä aikavälillä.

Suonensisäisen aortanpullistuman hoidon jälkeinen seuranta

Suonensisäisen hoidon jälkeen on suositeltavaa seurata potilasta säännöllisin radiologisin tutkimuksin. Näistä luotettavin tutkimusmetodi on tietokonetomografia suonensisäisen varjoaineen kanssa. Tällä kuvantamistekniikalla pystytään todentamaan sekä verisuoniproteesin kaikki osat, ajankohtainen sijainti että havainnoida verenvirtaus proteesin sisällä. Varjoaine on munuaisten toiminnalle vahingollista ja saattaa entisestään heikentää jo olemassa olevaa vajaatoimintaa. Lisäksi tietokonetomografiassa käytetään ionisoivaa röntgensäteilyä, joka voi usein toistuessaan teoreettisesti lisätä säteilyperäisten syöpien ilmentymistä. Tiettyjä

proteesikomplikaatiota voi hoitaa käyttämällä raskasmetallipitoista nk. verisuoniliimaa, kauppanimeltään Onyx®. Tämä, kuten muutkin metallit, aiheuttavat merkittäviä häiriöitä tietokonetomografiakuvissa ja heikentää huomattavissa määrin kuvien tulkinnallista tarkkuutta.

Tämä väitöskirja sisältää neljä osatyötä. Näissä arvioidaan uusia teknisiä mahdollisuuksia tehdä suonensisäisellä verisuoniproteesilla hoidettujen potilaiden jälkiseurantatutkimuksista turvallisempia ja mahdollisuuksia parantaa kuvanlaatua.

Osatyö I

Tarkoituksena oli vertailla laadullisesti kahta tietokonetomografista tutkimusmetodia. Uudempaa metodia käytettiin potilailla, joilla oli todettu munuaisten toiminnan heikentyminen ja standardimetodia munuaisterveillä potilailla. Munuaisten vajaatoiminnasta kärsivien potilaiden kuvaamisessa käytettiin 80 kVp jännitettä röntgenlaitteessa ja puolitettiin suonensisäinen varjoainemäärä. Munuaisterveiden potilaiden kuvaamisessa käytettiin 120 kVp jännitettä normaalin varjoainemäärän kanssa. Tutkimuksen tuloksena todettiin, että metodit ovat vertailukepoisia, mutta sillä rajoituksella, että 80 kVp tekniikka ei takaa riittävää kuvanlaatua huomattavan ylipainoisilla potilailla.

Osatyö II

Suonensisäisen verisuoniproteesin asentamisen jälkeisessä seurannassa käytetään kolmivaiheista tietokonetomografiatutkimusta. Ensimmäinen vaihe ajetaan ilman varjoainetta (TNC), toinen vaihe ajetaan välittömästi suonensisäisen varjoaineen annostelun jälkeen (nk valtimovaiheen kuvaus) ja kolmas vaihe muutaman kymmenen sekunnin kuluttua varjoaineen annostelemisesta (nk laskimovaiheen kuvaus). Tällä tavalla pystytään todentamaan kaikki mahdolliset proteesikomplikaatiot. Tämän osatyön tarkoituksena oli arvioida, voiko ensimmäisen kuvausvaiheen (TNC) ilman varjoainetta korvata keinotekoisella ei-varjoainekuvauksella (VNC) eli kuvilla, jotka rekonstruoidaan ensimmäisen varjoainevaiheen kuvista. Täten teoriassa kyettäisiin pienentämään merkittävästi säteilyn määrää yksittäisessä seurantatutkimuksessa. Tutkimuksen tuloksena oli kuitenkin, etteivät nämä keinotekoiset, laskennalliset ei-varjoainekuvat (VNC), olleet laadullisesti riittävän hyviä, eikä näitä voida suositella rutiininomaisessa seurantatutkimuksessa.

Osatyö III

Tässä työssä jatkettiin keinotekoisesti tuotettujen ei-varjoainekuvien (VNC) laadun tutkimista tuottamalla VNC kuvia ensimmäisestä valtimovaiheen kuvasarjasta sekä toisesta laskimovaiheen kuvasarjasta. Näitä molempia kuvasarjoja verrattiin ilman varjoainetta kuvattuun kuvasarjaan (TNC). Tutkimuksen tulos oli, että laskimovaiheen kuvauksesta tehdyissä VNC kuvissa oli kuvanlaatu riittävän lähellä

oikeasti ilman varjoainetta kuvattuun kuvasarjaan. Näin voitaisiin jättää yksi kuvausvaihe pois ja vähentää röntgensäteilyn määrää seurantakuvauksissa.

Osatyö IV

Tämän työn tarkoituksena oli soveltaa uutta metallista aiheutuvien kuvahäiriöiden vähentämiseksi kehitettyä matemaattista häiriönvähennyssuodatinta (iMAR) tietokonetomografiassa potilailla, joita oli hoidettu Onyx® verisuoniliimalla. Tutkimuksessa vertailtiin kuvausta ilman häiriönvähennyssuodatinta sekä vastaavia kuvia, joissa oli käytetty iMAR:ia. Tutkimus näyttää, että iMAR vähentää merkittävästi metallista aiheutuvia kuvantamishäiriötä ja voi pelastaa koko tutkimuksen diagnostisen varmuuden.

Acknowledgments

I want to express my sincere gratitude to all colleagues, friends, and family members who have contributed to, and supported me in my work with this thesis in so many ways:

I have had the best group of scientific supervisors I could ever wish for;

Johan Wasselius, associate professor, my main supervisor, for your total commitment and support pushing me to go on through the darkest time of scientific despair. You have a great mind of visions and a great sense of humour.

Marcus Söderberg, associate professor, my co-supervisor and brightest technical support. Thank you for your patience in explaining all the CT related details which are so basic to you but more complex to me. Thank you for all comments and quick replies in spite of being the father of a small baby and having such a busy daily life.

Anders Gottsäter, professor, my co-supervisor helping me to focus the essential matters in my scientific articles and put a skeleton to this book.

Ulf Nyman, associate professor, starting my scientific career and preparing me for the half-time review.

Peter Höglund, associate professor, my co-writer and statistical supervisor. Thank you for so many hours of delightful discussions on complex statistical questions!

Katarina Björses, my co-writer and true Finnish colleague! I want to thank for all support you gave me when landing in the southern part of Sweden called Skåne, and when my Swedish language was still so shaky.

Moncef Zarrouk, associate professor, helping me with SPSS and digging deeper into the mystery of vascular anomalies. You are a multiprofessional team in one person!

Nuno Dias and **Björn Sonesson** associate professors. You have introduced me to the most complex endovascular treatments one can imagine.

To my colleagues at **Kärlcentrum**, the previous ones and the present ones. It is just so delightful to work with you all!

To the professional **staff** at the **endovascular unit**. Thank you for all support and understanding during my process.

Kjerstin Ädel-Malmborg, You are the master of organization! Thank you for taking care of so many practical details to make my thesis defence possible!

Elisabeth Andersson, Shirin Atroushi, Ying Ydrefelt, radiological technicians for your valuable help saving the CT data for my studies.

Hanni Laura Aaltonen, for sharing your time and room for numerous discussions, relieving both clinical and scientific frustration. You managed to take a step ahead of me!

Raija and Aimo Lindfors, my dear mother and father. Thank you for believing in me. You have given me the best basis for my life, a safe and inspiring childhood.

Erik Rahlén, my love. You came into my life during the most intense time. Thank you for sharing life with me.

Olivia and Max Lehti, my precious children. I am so proud of you two! You have grown up into great young adults during my scientific process. I wish I could show that it is worth finding your dreams and strive for them. I love you both!

References

1. McGregor JC, Pollock JG, Anton HC. The value of ultrasonography in the diagnosis of abdominal aortic aneurysm. Scott Med J. 1975;20(3):133-7.
2. Johnston KW, Rutherford RB, Tilson MD, Shah DM, Hollier L, Stanley JC. Suggested standards for reporting on arterial aneurysms. Subcommittee on Reporting Standards for Arterial Aneurysms, Ad Hoc Committee on Reporting Standards, Society for Vascular Surgery and North American Chapter, International Society for Cardiovascular Surgery. J Vasc Surg. 1991;13(3):452-8.
3. Greenhalgh RM, Brown LC, Kwong GP, Powell JT, Thompson SG, participants Et. Comparison of endovascular aneurysm repair with open repair in patients with abdominal aortic aneurysm (EVAR trial 1), 30-day operative mortality results: randomised controlled trial. Lancet. 2004;364(9437):843-8.
4. Prinssen M, Verhoeven EL, Buth J, Cuypers PW, van Sambeek MR, Balm R, et al. A randomized trial comparing conventional and endovascular repair of abdominal aortic aneurysms. N Engl J Med. 2004;351(16):1607-18.
5. De Bruin JL, Baas AF, Buth J, Prinssen M, Verhoeven EL, Cuypers PW, et al. Long-term outcome of open or endovascular repair of abdominal aortic aneurysm. N Engl J Med. 2010;362(20):1881-9.
6. Lederle FA, Freischlag JA, Kyriakides TC, Padberg FT, Jr., Matsumura JS, Kohler TR, et al. Outcomes following endovascular vs open repair of abdominal aortic aneurysm: a randomized trial. JAMA. 2009;302(14):1535-42.
7. Tornqvist P, Resch T. Endoleaks after EVAR and TEVAR: indications for treatment and techniques. J Cardiovasc Surg (Torino). 2014;55(2 Suppl 1):105-14.
8. Erbel R, Aboyans V, Boileau C, Bossone E, Bartolomeo RD, Eggebrecht H, et al. 2014 ESC Guidelines on the diagnosis and treatment of aortic diseases: Document covering acute and chronic aortic diseases of the thoracic and abdominal aorta of the adult. The Task Force for the Diagnosis and Treatment of Aortic Diseases of the European Society of Cardiology (ESC). Eur Heart J. 2014;35(41):2873-926.
9. Mehran R, Nikolsky E. Contrast-induced nephropathy: definition, epidemiology, and patients at risk. Kidney international Supplement. 2006(100):S11-5.
10. Kawatani Y, Kurobe H, Nakamura Y, Hori T, Kitagawa T. The ratio of contrast medium volume to estimated glomerular filtration rate as a predictor of contrast-induced nephropathy after endovascular aortic repair. J Med Invest. 2018;65(1.2):116-21.
11. Moll FL, Powell JT, Fraedrich G, Verzini F, Haulon S, Waltham M, et al. Management of abdominal aortic aneurysms clinical practice guidelines of the

European society for vascular surgery. Eur J Vasc Endovasc Surg. 2011;41 Suppl 1:S1-S58.

12. Scott RA, Wilson NM, Ashton HA, Kay DN. Influence of screening on the incidence of ruptured abdominal aortic aneurysm: 5-year results of a randomized controlled study. Br J Surg. 1995;82(8):1066-70.
13. Ashton HA, Buxton MJ, Day NE, Kim LG, Marteau TM, Scott RA, et al. The Multicentre Aneurysm Screening Study (MASS) into the effect of abdominal aortic aneurysm screening on mortality in men: a randomised controlled trial. Lancet. 2002;360(9345):1531-9.
14. Norman PE, Jamrozik K, Lawrence-Brown MM, Le MT, Spencer CA, Tuohy RJ, et al. Population based randomised controlled trial on impact of screening on mortality from abdominal aortic aneurysm. BMJ. 2004;329(7477):1259.
15. Taudorf M, Jensen LP, Vogt KC, Gronvall J, Schroeder TV, Lonn L. Endograft limb occlusion in EVAR: iliac tortuosity quantified by three different indices on the basis of preoperative CTA. Eur J Vasc Endovasc Surg. 2014;48(5):527-33.
16. Gimenez-Gaibar A, Gonzalez-Canas E, Solanich-Valldaura T, Herranz-Pinilla C, Rioja-Artal S, Ferraz-Huguet E. Could Preoperative Neck Anatomy Influence Follow-up of EVAR? Ann Vasc Surg. 2017;43:127-33.
17. Mahajan A, Barber M, Cumbie T, Filardo G, Shutze WP, Jr., Sass DM, et al. The Impact of Aneurysm Morphology and Anatomic Characteristics on Long-Term Survival after Endovascular Abdominal Aortic Aneurysm Repair. Ann Vasc Surg. 2016;34:75-83.
18. Gargiulo M, Gallitto E, Wattez H, Verzini F, Bianchini Massoni C, Loschi D, et al. Outcomes of endovascular aneurysm repair performed in abdominal aortic aneurysms with large infrarenal necks. J Vasc Surg. 2017;66(4):1065-72.
19. Bannazadeh M, Jenkins C, Forsyth A, Kramer J, Aggarwal A, Somerset AE, et al. Outcomes for concomitant common iliac artery aneurysms after endovascular abdominal aortic aneurysm repair. J Vasc Surg. 2017;66(5):1390-7.
20. Pitoulias GA, Valdivia AR, Hahtapornsawan S, Torsello G, Pitoulias AG, Austermann M, et al. Conical neck is strongly associated with proximal failure in standard endovascular aneurysm repair. J Vasc Surg. 2017;66(6):1686-95.
21. Gallitto E, Gargiulo M, Freyrie A, Bianchini Massoni C, Pini R, Mascoli C, et al. Results of standard suprarenal fixation endografts for abdominal aortic aneurysms with neck length </=10 mm in high-risk patients unfit for open repair and fenestrated endograft. J Vasc Surg. 2016;64(3):563-70 e1.
22. Kwon H, Han Y, Noh M, Gwon JG, Cho YP, Kwon TW. Impact of Shaggy Aorta in Patients with Abdominal Aortic Aneurysm Following Open or Endovascular Aneurysm Repair. Eur J Vasc Endovasc Surg. 2016;52(5):613-9.
23. Stacul F, van der Molen AJ, Reimer P, Webb JA, Thomsen HS, Morcos SK, et al. Contrast induced nephropathy: updated ESUR Contrast Media Safety Committee guidelines. European radiology. 2011;21(12):2527-41.
24. Piacentino F, Fontana F, Micieli C, Angeretti MG, Cardim LN, Coppola A, et al. Nonenhanced MRI Planning for Endovascular Repair of Abdominal Aortic

Aneurysms: Comparison With Contrast-Enhanced CT Angiography. Vasc Endovascular Surg. 2018;52(1):39-45.

25. Kent KC, Zwolak RM, Egorova NN, Riles TS, Manganaro A, Moskowitz AJ, et al. Analysis of risk factors for abdominal aortic aneurysm in a cohort of more than 3 million individuals. J Vasc Surg. 2010;52(3):539-48.
26. Lindholt JS, Juul S, Fasting H, Henneberg EW. Hospital costs and benefits of screening for abdominal aortic aneurysms. Results from a randomised population screening trial. Eur J Vasc Endovasc Surg. 2002;23(1):55-60.
27. Wanhainen A, Hultgren R, Linne A, Holst J, Gottsater A, Langenskiold M, et al. Outcome of the Swedish Nationwide Abdominal Aortic Aneurysm Screening Program. Circulation. 2016;134(16):1141-8.
28. Volodos NL, Karpovich IP, Shekhanin VE, Troian VI, Iakovenko LF. [A case of distant transfemoral endoprosthesis of the thoracic artery using a self-fixing synthetic prosthesis in traumatic aneurysm]. Grudn Khir. 1988(6):84-6.
29. Parodi JC, Palmaz JC, Barone HD. Transfemoral intraluminal graft implantation for abdominal aortic aneurysms. Ann Vasc Surg. 1991;5(6):491-9.
30. Seldinger SI. Catheter replacement of the needle in percutaneous arteriography; a new technique. Acta radiologica. 1953;39(5):368-76.
31. de la Motte L, Jensen LP, Vogt K, Kehlet H, Schroeder TV, Lonn L. Outcomes after elective aortic aneurysm repair: a nationwide Danish cohort study 2007-2010. Eur J Vasc Endovasc Surg. 2013;46(1):57-64.
32. van Keulen JW, Moll FL, van Herwaarden JA. Tips and techniques for optimal stent graft placement in angulated aneurysm necks. J Vasc Surg. 2010;52(4):1081-6.
33. Tsilimparis N, Debus SE, Biehl M, Spanos K, Larena-Avellaneda A, Wipper S, et al. Fenestrated-branched endografts and visceral debranching plus stenting (hybrid) for complex aortic aneurysm repair. J Vasc Surg. 2018;67(6):1684-9.
34. Patel SR, Allen C, Grima MJ, Brownrigg JRW, Patterson BO, Holt PJE, et al. A Systematic Review of Predictors of Reintervention After EVAR: Guidance for Risk-Stratified Surveillance. Vasc Endovascular Surg. 2017;51(6):417-28.
35. White GH, Yu W, May J. Endoleak--a proposed new terminology to describe incomplete aneurysm exclusion by an endoluminal graft. J Endovasc Surg. 1996;3(1):124-5.
36. Liaw JV, Clark M, Gibbs R, Jenkins M, Cheshire N, Hamady M. Update: Complications and management of infrarenal EVAR. European journal of radiology. 2009;71(3):541-51.
37. Wilt TJ, Lederle FA, Macdonald R, Jonk YC, Rector TS, Kane RL. Comparison of endovascular and open surgical repairs for abdominal aortic aneurysm. Evid Rep Technol Assess (Full Rep). 2006(144):1-113.
38. Martin ML, Dolmatch BL, Fry PD, Machan LS. Treatment of type II endoleaks with Onyx. Journal of vascular and interventional radiology : JVIR. 2001;12(5):629-32.
39. Jouhannet C, Alsac JM, Julia P, Sapoval M, El Batti S, Di Primio M, et al. Reinterventions for type 2 endoleaks with enlargement of the aneurismal sac after

endovascular treatment of abdominal aortic aneurysms. Ann Vasc Surg. 2014;28(1):192-200.

40. Fearn S, Lawrence-Brown MM, Semmens JB, Hartley D. Follow-up after endovascular aortic aneurysm repair: the plain radiograph has an essential role in surveillance. J Endovasc Ther. 2003;10(5):894-901.
41. d'Audiffret A, Desgranges P, Kobeiter DH, Becquemin JP. Follow-up evaluation of endoluminally treated abdominal aortic aneurysms with duplex ultrasonography: validation with computed tomography. J Vasc Surg. 2001;33(1):42-50.
42. Bredahl KK, Taudorf M, Lonn L, Vogt KC, Sillesen H, Eiberg JP. Contrast Enhanced Ultrasound can Replace Computed Tomography Angiography for Surveillance After Endovascular Aortic Aneurysm Repair. Eur J Vasc Endovasc Surg. 2016;52(6):729-34.
43. Bredahl K, Taudorf M, Long A, Lonn L, Rouet L, Ardon R, et al. Three-dimensional ultrasound improves the accuracy of diameter measurement of the residual sac in EVAR patients. Eur J Vasc Endovasc Surg. 2013;46(5):525-32.
44. Rubenthaler J, Reiser M, Cantisani V, Rjosk-Dendorfer D, Clevert DA. The value of contrast-enhanced ultrasound (CEUS) using a high-end ultrasound system in the characterization of endoleaks after endovascular aortic repair (EVAR). Clin Hemorheol Microcirc. 2017;66(4):283-92.
45. Stavropoulos SW, Clark TW, Carpenter JP, Fairman RM, Litt H, Velazquez OC, et al. Use of CT angiography to classify endoleaks after endovascular repair of abdominal aortic aneurysms. Journal of vascular and interventional radiology : JVIR. 2005;16(5):663-7.
46. Ayuso JR, de Caralt TM, Pages M, Riambau V, Ayuso C, Sanchez M, et al. MRA is useful as a follow-up technique after endovascular repair of aortic aneurysms with nitinol endoprostheses. J Magn Reson Imaging. 2004;20(5):803-10.
47. Klemm T, Duda S, Machann J, Seekamp-Rahn K, Schnieder L, Claussen CD, et al. MR imaging in the presence of vascular stents: A systematic assessment of artifacts for various stent orientations, sequence types, and field strengths. J Magn Reson Imaging. 2000;12(4):606-15.
48. van der Laan MJ, Bartels LW, Viergever MA, Blankensteijn JD. Computed tomography versus magnetic resonance imaging of endoleaks after EVAR. Eur J Vasc Endovasc Surg. 2006;32(4):361-5.
49. van Prehn J, van Herwaarden JA, Vincken KL, Verhagen HJ, Moll FL, Bartels LW. Asymmetric aortic expansion of the aneurysm neck: analysis and visualization of shape changes with electrocardiogram-gated magnetic resonance imaging. J Vasc Surg. 2009;49(6):1395-402.
50. Hernesniemi JA, Vanni V, Hakala T. The prevalence of abdominal aortic aneurysm is consistently high among patients with coronary artery disease. J Vasc Surg. 2015;62(1):232-40 e3.
51. Durieux R, Van Damme H, Labropoulos N, Yazici A, Legrand V, Albert A, et al. High prevalence of abdominal aortic aneurysm in patients with three-vessel coronary artery disease. Eur J Vasc Endovasc Surg. 2014;47(3):273-8.

52. Altobelli E, Rapacchietta L, Profeta VF, Fagnano R. Risk Factors for Abdominal Aortic Aneurysm in Population-Based Studies: A Systematic Review and Meta-Analysis. Int J Environ Res Public Health. 2018;15(12).
53. Forsdahl SH, Singh K, Solberg S, Jacobsen BK. Risk factors for abdominal aortic aneurysms: a 7-year prospective study: the Tromso Study, 1994-2001. Circulation. 2009;119(16):2202-8.
54. Lederle FA, Johnson GR, Wilson SE, Chute EP, Littooy FN, Bandyk D, et al. Prevalence and associations of abdominal aortic aneurysm detected through screening. Aneurysm Detection and Management (ADAM) Veterans Affairs Cooperative Study Group. Ann Intern Med. 1997;126(6):441-9.
55. Ronco C, Haapio M, House AA, Anavekar N, Bellomo R. Cardiorenal syndrome. Journal of the American College of Cardiology. 2008;52(19):1527-39.
56. Flohr TG, McCollough CH, Bruder H, Petersilka M, Gruber K, Suss C, et al. First performance evaluation of a dual-source CT (DSCT) system. European radiology. 2006;16(2):256-68.
57. Graser A, Johnson TR, Chandarana H, Macari M. Dual energy CT: preliminary observations and potential clinical applications in the abdomen. European radiology. 2009;19(1):13-23.
58. Meyer BC, Werncke T, Hopfenmuller W, Raatschen HJ, Wolf KJ, Albrecht T. Dual energy CT of peripheral arteries: effect of automatic bone and plaque removal on image quality and grading of stenoses. European journal of radiology. 2008;68(3):414-22.
59. Johnson TR, Krauss B, Sedlmair M, Grasruck M, Bruder H, Morhard D, et al. Material differentiation by dual energy CT: initial experience. European radiology. 2007;17(6):1510-7.
60. McCollough CH, Leng S, Yu L, Fletcher JG. Dual- and Multi-Energy CT: Principles, Technical Approaches, and Clinical Applications. Radiology. 2015;276(3):637-53.
61. Si-Mohamed S, Bar-Ness D, Sigovan M, Cormode DP, Coulon P, Coche E, et al. Review of an initial experience with an experimental spectral photon-counting computed tomography system. Nuclear Instruments and Methods in Physics Research Section A: Accelerators, Spectrometers, Detectors and Associated Equipment. 2017;873:27-35.
62. Dangelmaier J, Bar-Ness D, Daerr H, Muenzel D, Si-Mohamed S, Ehn S, et al. Experimental feasibility of spectral photon-counting computed tomography with two contrast agents for the detection of endoleaks following endovascular aortic repair. European radiology. 2018;28(8):3318-25.
63. Goldman LW. Principles of CT: radiation dose and image quality. J Nucl Med Technol. 2007;35(4):213-25; quiz 26-8.
64. Goldman LW. Principles of CT and CT technology. J Nucl Med Technol. 2007;35(3):115-28; quiz 29-30.
65. Barrett JF, Keat N. Artifacts in CT: recognition and avoidance. Radiographics. 2004;24(6):1679-91.
66. Hansson SO. ALARA: What is Reasonably Achievable? Social and Ethical Aspects of Radiation Risk Management. Radioactivity in the Environment2013. p. 143-55.

67. Willemink MJ, Leiner T, de Jong PA, de Heer LM, Nievelstein RA, Schilham AM, et al. Iterative reconstruction techniques for computed tomography part 2: initial results in dose reduction and image quality. European radiology. 2013;23(6):1632-42.
68. Pontana F, Pagniez J, Flohr T, Faivre JB, Duhamel A, Remy J, et al. Chest computed tomography using iterative reconstruction vs filtered back projection (Part 1): Evaluation of image noise reduction in 32 patients. European radiology. 2011;21(3):627-35.
69. Rajiah P, Schoenhagen P, Mehta D, Ivanc T, Lieber M, Soufan K, et al. Low-dose, wide-detector array thoracic aortic CT angiography using an iterative reconstruction technique results in improved image quality with lower noise and fewer artifacts. J Cardiovasc Comput Tomogr. 2012;6(3):205-13.
70. Kataria B, Althen JN, Smedby O, Persson A, Sokjer H, Sandborg M. Assessment of image quality in abdominal CT: potential dose reduction with model-based iterative reconstruction. European radiology. 2018;28(6):2464-73.
71. Brink JA, Heiken JP, Wang G, McEnery KW, Schlueter FJ, Vannier MW. Helical CT: principles and technical considerations. Radiographics. 1994;14(4):887-93.
72. Willemink MJ, de Jong PA, Leiner T, de Heer LM, Nievelstein RA, Budde RP, et al. Iterative reconstruction techniques for computed tomography Part 1: technical principles. European radiology. 2013;23(6):1623-31.
73. Beister M, Kolditz D, Kalender WA. Iterative reconstruction methods in X-ray CT. Physica medica : PM : an international journal devoted to the applications of physics to medicine and biology : official journal of the Italian Association of Biomedical Physics. 2012;28(2):94-108.
74. Toepker M, Moritz T, Krauss B, Weber M, Euller G, Mang T, et al. Virtual non-contrast in second-generation, dual-energy computed tomography: reliability of attenuation values. European journal of radiology. 2012;81(3):e398-405.
75. Muller-Wille R, Borgmann T, Wohlgemuth WA, Zeman F, Pfister K, Jung EM, et al. Dual-energy computed tomography after endovascular aortic aneurysm repair: the role of hard plaque imaging for endoleak detection. European radiology. 2014;24(10):2449-57.
76. Katsura M, Sato J, Akahane M, Kunimatsu A, Abe O. Current and Novel Techniques for Metal Artifact Reduction at CT: Practical Guide for Radiologists. Radiographics. 2018;38(2):450-61.
77. Kachelriess M, Watzke O, Kalender WA. Generalized multi-dimensional adaptive filtering for conventional and spiral single-slice, multi-slice, and cone-beam CT. Medical physics. 2001;28(4):475-90.
78. Lemmens C, Faul D, Nuyts J. Suppression of metal artifacts in CT using a reconstruction procedure that combines MAP and projection completion. IEEE Trans Med Imaging. 2009;28(2):250-60.
79. Wang G, Snyder DL, O'Sullivan JA, Vannier MW. Iterative deblurring for CT metal artifact reduction. IEEE Trans Med Imaging. 1996;15(5):657-64.

80. Meyer E, Raupach R, Lell M, Schmidt B, Kachelriess M. Normalized metal artifact reduction (NMAR) in computed tomography. Medical physics. 2010;37(10):5482-93.
81. Meyer E, Raupach R, Lell M, Schmidt B, Kachelriess M. Frequency split metal artifact reduction (FSMAR) in computed tomography. Medical physics. 2012;39(4):1904-16.
82. Kachelriess M. Iterative Metal Artifact Reduction (iMAR): Technical Principles and Clinical Results in Radiation Therapy. 2014.
83. The 2007 Recommendations of the International Commission on Radiological Protection. ICRP publication 103. Ann ICRP. 2007;37(2-4):1-332.
84. Borjesson S, Hakansson M, Bath M, Kheddache S, Svensson S, Tingberg A, et al. A software tool for increased efficiency in observer performance studies in radiology. Radiation protection dosimetry. 2005;114(1-3):45-52.
85. Hakansson M, Svensson S, Zachrisson S, Svalkvist A, Bath M, Mansson LG. VIEWDEX: an efficient and easy-to-use software for observer performance studies. Radiation protection dosimetry. 2010;139(1-3):42-51.
86. Rankin SC. CT angiography. European radiology. 1999;9(2):297-310.
87. Nyman U, Bjorkdahl P, Olsson ML, Gunnarsson M, Goldman B. Low-dose radiation with 80-kVp computed tomography to diagnose pulmonary embolism: a feasibility study. Acta radiologica. 2012;53(9):1004-13.
88. Kristiansson M, Holmquist F, Nyman U. Ultralow contrast medium doses at CT to diagnose pulmonary embolism in patients with moderate to severe renal impairment: a feasibility study. European radiology. 2010;20(6):1321-30.
89. Mourits MM, Nijhof WH, van Leuken MH, Jager GJ, Rutten MJ. Reducing contrast medium volume and tube voltage in CT angiography of the pulmonary artery. Clin Radiol. 2016;71(6):615 e7- e13.
90. Szucs-Farkas Z, Schibler F, Cullmann J, Torrente JC, Patak MA, Raible S, et al. Diagnostic accuracy of pulmonary CT angiography at low tube voltage: intraindividual comparison of a normal-dose protocol at 120 kVp and a low-dose protocol at 80 kVp using reduced amount of contrast medium in a simulation study. AJR American journal of roentgenology. 2011;197(5):W852-9.
91. Wintersperger B, Jakobs T, Herzog P, Schaller S, Nikolaou K, Suess C, et al. Aorto-iliac multidetector-row CT angiography with low kV settings: improved vessel enhancement and simultaneous reduction of radiation dose. European radiology. 2005;15(2):334-41.
92. Canstein C. Reduction of contrast agent dose at low kV settings. Whitepaper. 2017;Siemens Healthineers.
93. Wellenberg RH, Boomsma MF, van Osch JA, Vlassenbroek A, Milles J, Edens MA, et al. Computed Tomography Imaging of a Hip Prosthesis Using Iterative Model-Based Reconstruction and Orthopaedic Metal Artefact Reduction: A Quantitative Analysis. J Comput Assist Tomogr. 2016;40(6):971-8.
94. Korpics M, Surucu M, Mescioglu I, Alite F, Block AM, Choi M, et al. Observer Evaluation of a Metal Artifact Reduction Algorithm Applied to Head and Neck Cone

Beam Computed Tomographic Images. Int J Radiat Oncol Biol Phys. 2016;96(4):897-904.

95. Aissa J, Thomas C, Sawicki LM, Caspers J, Kropil P, Antoch G, et al. Iterative metal artefact reduction in CT: can dedicated algorithms improve image quality after spinal instrumentation? Clin Radiol. 2017;72(5):428 e7- e12.
96. Clevert DA, Helck A, D'Anastasi M, Gurtler V, Sommer WH, Meimarakis G, et al. Improving the follow up after EVAR by using ultrasound image fusion of CEUS and MS-CT. Clin Hemorheol Microcirc. 2011;49(1-4):91-104.
97. Pineda DM, Phillips ZM, Calligaro KD, Krol E, Dougherty MJ, Troutman DA, et al. The fate of endovascular aortic aneurysm repair after 5 years monitored with duplex ultrasound imaging. J Vasc Surg. 2017;66(2):392-5.
98. Andersen RM, Henriksen DP, Mafi HM, Langfeldt S, Budtz-Lilly J, Graumann O. A Long-Time Follow-Up Study of a Single-Center Endovascular Aneurysm Repair (Evar) Endoleak Outcomes. Vasc Endovascular Surg. 2018;52(7):505-11.

Printed by Media-Tryck, Lund 2019 NORDIC SWAN ECOLABEL 3041 0903

Diagnostic quality in computed tomography angiography after EVAR

Leena Lehti is a medical doctor specialized in clinical radiology. She studied medicine at Tampere University (1991-1997) and became a specialist in radiology at Helsinki University in 2007. Since 2009, she works as an interventional radiologist at Malmö Vascular Center, a clinic with a multi-professional team.

LUND UNIVERSITY

FACULTY OF MEDICINE

Department of Diagnostic Radiology
Institution of Clinical Sciences, Lund

Lund University, Faculty of Medicine
Doctoral Dissertation Series 2019:62
ISBN 978-91-7619-791-2
ISSN 1652-8220